Geoscience Frontiers 11 (2020) 965–988

HOSTED BY

ELSEVIER

Contents lists available at ScienceDirect

Geoscience Frontiers

journal homepage: www.elsevier.com/locate/gsf

Research Paper

Organo-petrographic and geochemical characteristics of Gurha lignite deposits, Rajasthan, India: Insights into the palaeovegetation, palaeoenvironment and hydrocarbon source rock potential

Runcie Paul Mathews [a], Bhagwan D. Singh [a], Vikram Partap Singh [a,*], Alpana Singh [a], Hukam Singh [a], Mahesh Shivanna [a], Suryendu Dutta [b], Vinod A. Mendhe [c], Rimpy Chetia [a]

[a] DST- Birbal Sahni Institute of Palaeosciences, Lucknow, 226007, India
[b] Department of Earth Sciences, Indian Institute of Technology Bombay, Mumbai, 400076, India
[c] CSIR-Central Institute of Mining and Fuel Research, Dhanbad, 826015, India

ARTICLE INFO

Handling Editor: Kristoffer Szilas

Keywords:
Palynofacies
Biomarkers
Rock-Eval
Palaeocene deposits
Bikaner-Nagaur Basin

ABSTRACT

The sedimentary sequence containing lignite deposits in Gurha quarry of the Bikaner-Nagaur Basin (Rajasthan) has been investigated. The samples from lignite and allied shale horizons were evaluated for petrographical, palynological, palynofacies and organic geochemical inferences, to depict the source flora and to reconstruct the palaeodepositional conditions prevailed during the sedimentation. An assessment for the hydrocarbon generation potential of these deposits has also been made. The results revealed the dominance of huminite macerals and phytoclasts organic matter (OM) indicating the existence of forested vegetation in the vicinity of the depositional site. A relatively high terrigenous/aquatic ratio (TAR) and the carbon preference index (CPI) are also suggesting the contribution of higher plants in the peat formation. However, the *n*-alkane distributions, maximizing at *n*-C_{17} and *n*-C_{29}, showed inputs from the algal communities along with the higher plant derived organic matters. Recovered palynomorphs of the families Onagraceae, Meliaceae, Arecaceae, Rhizophoraceae, Rubiaceae, Ctenolophonaceae, etc. together with oleanene and ursane types of triterpenoids suggest the contribution from angiosperms source vegetation. Interestingly, the presence of Araucareaceae and Podocarpaceae pollen grains shows the existence of gymnosperms vegetation. Further, the presence of tetracyclic diterpanes; demethylated ent-beyerane, sandaracopimarane, pimarane, and Kaurane type of compounds confirms the contribution of conifers. The variation in the values of the coefficient of non-equality (H: 0.68%–7.56%), the standard deviation (δ: 0.04%–0.16%) and the coefficient of variability (V: 16.10%–46.47%), also shows the heterogeneity in the source organic matter.

The various petrographical indices, palynological entities, and geochemical parameters indicate that the peat-forming vegetation was accumulated under a mixed environment and fluctuating hydrological settings. The interpretation of palynofacies data on APP (Amorphous organic matter-Phytoclast-Palynomorphs) diagram suggests that the accumulation of organic matter occurred in a dysoxic-suboxic condition in a proximal (to land) setting with the shift to an anoxic condition in distal setting towards the termination of sedimentation. The huminite (ulminite) reflectance (R_r) values (av. 0.28%) showed a good relationship with average T_{max} value (414 °C), suggesting the immaturity. The TOC content ranges of 13–59 wt.%, and HI values vary between 101 and 546 mg HC/g TOC in the studied samples. Collectively, the studied lignite and shale samples have the admixed kerogens (Type III–II) and exhibit the ability to generate the gaseous to oil hydrocarbons upon maturation.

1. Introduction

Lignite/coal is a highly composite blend of plant remains which has been transformed by various microbial and diagenetic activities (Hatcher and Clifford, 1997; Wilkins and George, 2002). Therefore, the organic matter (OM) preserve in the sediments (lignite, coal, shale, etc.) are

* Corresponding author.
E-mail address: vikram_chauhan@bsip.res.in (V.P. Singh).
Peer-review under responsibility of China University of Geosciences (Beijing).

https://doi.org/10.1016/j.gsf.2019.10.002
Received 13 June 2019; Received in revised form 3 September 2019; Accepted 12 October 2019
Available online 6 November 2019

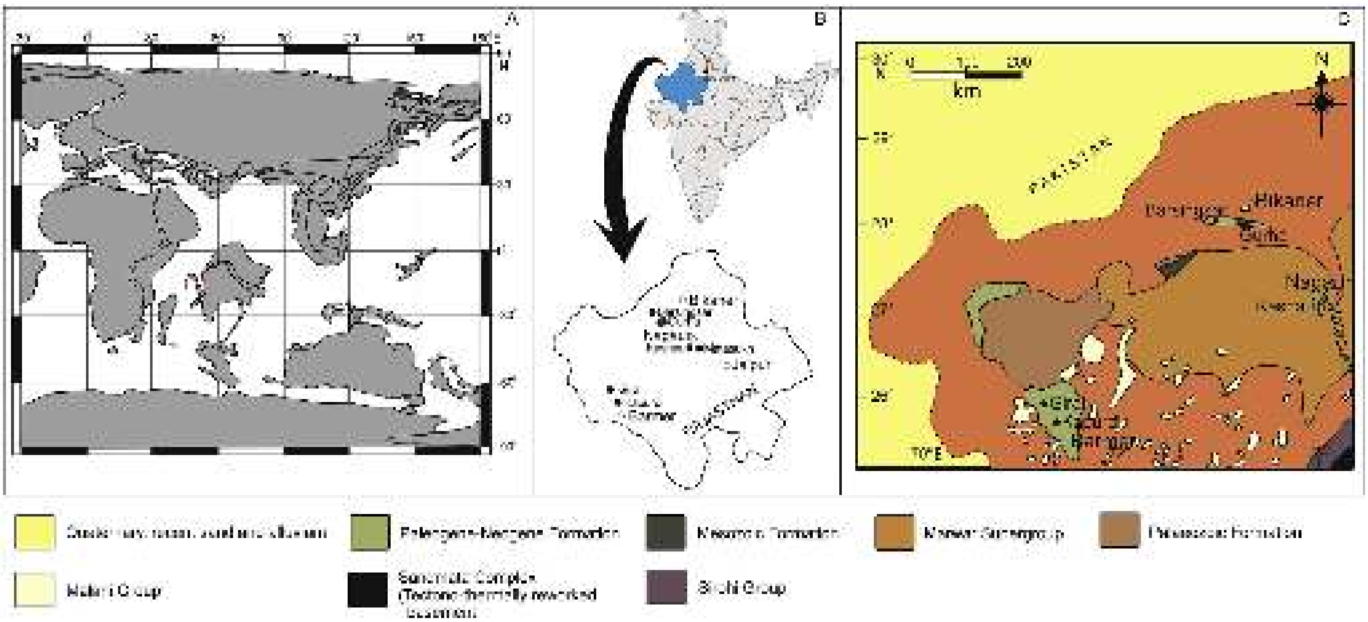

Fig. 1. (A) Palaeogeographical reconstruction map of Indian Subcontinent (western part encircled) during Palaeocene (66 Ma) (www.odsn.de/odsn/index.html). (B) Location map of Gurha lignite mine in Rajasthan state, northwestern India. (C) Generalized geological map of the study area.

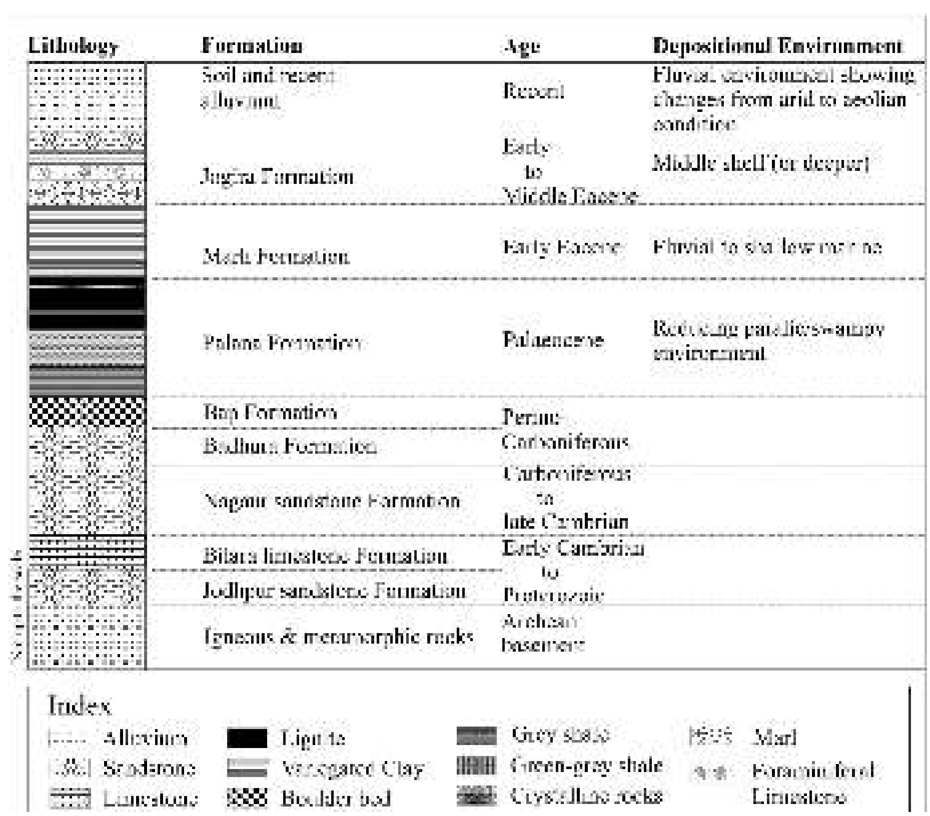

Fig. 2. A generalized lithostratigraphic succession of Bikaner-Nagaur Basin, northwestern India.

thought to reflect the conditions prevailing during the time of their deposition and the botanical framework of the areas. In the investigation of these organic-rich deposits, organic petrography is widely considered as one of the best methods to deduce the palaeodepositional conditions, besides providing valuable inputs about the source vegetation, maturity and hydrocarbon generation potential of the OM (Taylor et al., 1998; Bechtel et al., 2005; Dai et al., 2007; Zdravkov et al., 2011; Suárez-Ruiz et al., 2012; Singh et al., 2017a, b, c; and many others).

Organic facies (particulate organic matter) reflects the information about the palaeobotanical framework, the original environment and depositional conditions of the source area. Thus, these facies has been widely used to describe the palaeovegetation and to understand the

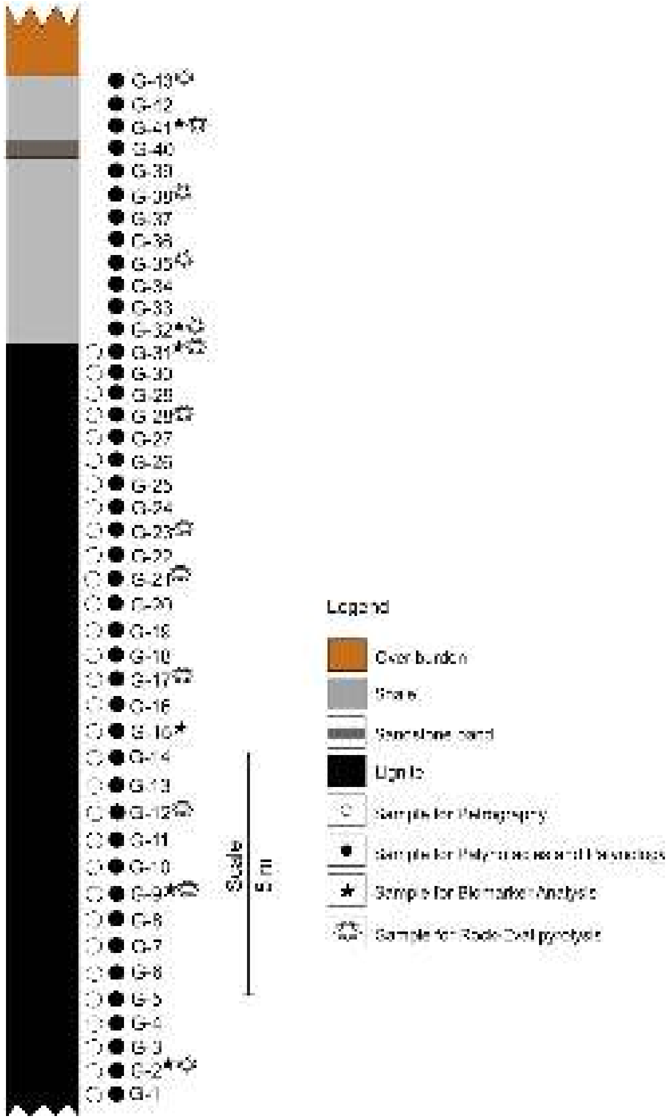

Fig. 3. Litholog of the studied Gurha lignite mine section showing the lithounits and samples.

evolution of peat-swamps (Tyson, 1995; Batten, 1996; Mendonça Filho et al., 2011, 2012; Singh et al., 2013, 2017a, b, c). The organic facies study also indicate the potenital of sedimentary rock to generate hydrocarbons (Singh et al., 2017a, b). Further, the assessment of palynomorphs affinity to their parent plants and their associated habitats can help in evaluating palaeovegetation and biome evolution. Their abundant production provides them with the feasibility of getting preserved in almost every kind of environment and provides a large dataset with high statistic fidelity. The palynology can also be applied for establishing the stratigraphy, and phytogeographic and palaeoclimatic interpretations (Singh et al., 1992; Ampaiwan et al., 2003; Hoorn et al., 2012).

In addition, Gas Chromatography-Mass Spectrometry (GC-MS) is considered as a useful technique with which the chemical compositions of the organic matter can be easily deciphered (Nip et al., 1985; Hatcher and Clifford, 1997; Dutta et al., 2011). The contributions of different types of plant produce various types of biopolymers. These biopolymers have been contributed through the original organic matters, and the degree of coalification determines the chemical structure of coal/lignite.

The Palaeocene successions in the western part of Indian subcontinent (South Asia) have a significant role in understanding the faunal and floral relationships on the drifting of the Indian plate (Fig. 1A) with respect to its Gondwanan continental associations (Singh et al., 2011, 2015a; Paul et al., 2015, see ref. for details). The lignite deposits of Bikaner sub-basin in northwestern India are associated with the Palana Formation of Palaeocene age (~66–56 Ma), and being excavated at Gurha and Barsingsar areas in Bikaner district of Rajasthan State (Fig. 1B). The lignite deposts of the basin were studied by various researchers to understand the palynological attributes of the succession (Sah and Kar, 1974; Singh and Dogra, 1988; Kar, 1995, 1996; Ambwani and Singh, 1996; Kar and Sharma, 2001; Singh et al., 2017c and many others). Shukla et al. (2014) suggested a cool temperate climate for the Gurha succession, based on the CLAMP (Climate Leaf Analysis Multivariant Program) technique on fossil leaves. However, Naafs et al. (2018) found high values of isoGDGT-5, and the $MAAT_{peat}$ (mean annual air temperature) in the lignites deposits of India (~0–5°N) ranges of (28–29) °C ± 4.7 °C, higher than any other low latitudes basins, suggesting a much hotter (as estimated earlier) terrestrial region during the early Palaeogene. The preliminary data about the characterization and hydrocarbon potential for these lignites has been provided by Singh et al. (2015b, 2016), Singh and Kumar (2018) and Rajak et al. (2019). Paul and Dutta (2016) performed the molecular characterization of fossil resin from the Gurha lignite mine. Kumar et al. (2016), Shukla and Mehrotra (2018), and Shukla et al. (2018) on the basis of palynology and nearest living relatives (NLRs), respectively) suggested the occurrences of frequent wildfires and a strong rainfall seasonality for a near coastal tropical evergreen vegetation of Gurha mine.

Building upon and integrating these research results can lead to more confident reconstruction of the palaeovegetation and environment. Therefore, the present multidisciplinary investigation (on new set of samples) has been taken up for a better understanding of botanical origin, nature, composition and depositional settings of the Gurha lignites, besides attempting to estimate the hydrocarbon generation potential of these Palaeocene deposits. It is supplementary to the categorization of the DGH, MoPNG (India) that the Bikaner-Nagaur comes under the productive Basin-I category.

2. Geology and lignite deposits

Rajasthan State as a part of Indian shield consists of sedimentary records covering a time span from early Archaean to Holocene. The distinct basins viz. Bikaner-Nagaur, Barmer and Jaisalmer basins, developed as a result of the intracratonic sedimentation covering an area of about 120,000 km^2 (Bhowmick, 2008). The basin (Neoproterozoic–early Palaeozoic) covers an area of 30,000 km^2 in the districts of Bikaner and Nagaur (Prasad et al., 2010). It (basin) comprised of Delhi metamorphites and MIS (Malani Igneous Suite) and is the largest of the basins in western Rajasthan. The overall sedimentary thickness is approx. 2100 m in the basin (Raju et al., 2014). The generalized stratigraphic succession of the Bikaner-Nagaur Basin is presented in Fig. 2.

The Bikaner-Nagaur Basin display thick late Palaeozoic deposits, followed by a relatively thin Mesozoic and Cenozoic sediments. The Cenozoic deposits show a large extension of over 1700 km^2 (Fig. 1C). Further, the Cenozoic era has been initiated by the lignite-bearing Palana Formation. The formation is well exposed in Barsingsar and Gurha mines, belonging to Palana-Kolayat sub-basin in the North, and in Kasnau-Matasukh mine belonging to Nagaur-Merta sub-basin, in the south of the Bikaner-Nagaur Basin. The Palana Formation (av. thickness 200 m) is composed of sandstone, silt stone, sandy clay, clay, carbonaceous shale, lignite and minor limestone (Sinha-Roy et al., 1998; Singh et al., 2015b). The Marh Formation of argillaceous and ferruginous facies overlies the Palana Formation. The Cenozoic sedimentation in the basin ended up with the deposition of Jogira Formation having marine signatures.

The Gurha (East) lignite mine (27°55′N, 72°58′E) is situated about 20 km northwest of Kolayat town in the Bikaner district. The Gurha mine contains about 38 million tonnes of reserves, and the lignite seams are

Table 1
Maceral contents (vol.%), mineral matter content (vol.%), ulminite reflectance (Rr, in %) and petrographic indices (GI, TPI, GWI, VI) of Gurha lignites.

Sample No.	G – 1	G – 2	G – 3	G – 4	G – 5	G – 6	G – 7	G – 8	G – 9	G – 10	G – 11	G – 12	G – 13	G – 14	G – 15	G – 16	G – 17
Macerals																	
Huminite (H)	59	52	49	60	61	53	68	69	48	53	62	47	59	53	72	39	61
Telohuminite	10	34	6	41	18	19	32	21	27	19	11	19	13	18	44	24	5
Textinite	1	1	0	2	2	1	1	0	0	0	0	0	0	0	2	0	0
Ulminite	9	33	6	39	16	19	31	21	27	19	11	19	13	18	43	24	5
Detrohuminite	48	15	43	17	38	32	33	47	21	33	51	27	47	35	24	13	55
Attrinite	2	2	34	5	31	7	5	11	8	13	0	5	3	10	13	6	4
Densinite	46	13	9	12	8	25	27	36	13	20	55	23	44	25	11	7	51
Gelohuminite	1	3	1	3	5	1	4	1	0	1	1	1	0	1	3	3	1
Corpohuminite	1	3	1	3	5	1	4	1	0	1	1	1	0	1	3	3	1
Liptinite (L)	**11**	**14**	**6**	**8**	**10**	**16**	**15**	**10**	**8**	**9**	**12**	**6**	**18**	**15**	**11**	**12**	**17**
Sporinite	2	2	1	1	3	2	5	0	1	1	1	1	0	2	2	3	1
Cutinite	1	3	1	3	1	3	1	1	5	1	1	1	0	3	2	3	0
Suberinite	0	0	0	0	0	0	0	0	0	0	1	0	0	0	0	0	0
Resinite	5	2	2	3	2	7	3	4	2	4	4	1	7	3	4	5	11
Alginite	0	0	0	0	0	0	0	0	0	0	0	0	3	0	0	0	0
Bituminite	0	3	0	0	0	0	0	0	0	0	0	0	0	0	0	0	0
Liptodetrinite	4	5	3	1	4	3	6	5	1	3	5	2	9	6	3	2	5
Inertinite (I)	**17**	**24**	**39**	**26**	**20**	**29**	**16**	**15**	**38**	**35**	**22**	**42**	**9**	**28**	**10**	**45**	**22**
Semifusinite	10	7	20	7	10	6	4	8	8	19	11	16	5	12	3	12	8
Fusinite	2	0	0	1	0	1	8	1	0	1	5	3	2	0	0	0	6
Funginite	0	6	3	3	3	2	2	1	7	1	1	4	0	0	6	9	2
Inertodetrinite	6	11	16	15	7	20	2	5	22	14	5	19	2	16	2	24	6
Mineral Matter (TOTAL)	**13**	**9**	**5**	**6**	**9**	**3**	**1**	**6**	**6**	**3**	**4**	**5**	**14**	**4**	**8**	**5**	**1**
Others	11	6	1	6	2	2	1	6	6	2	4	5	13	4	6	5	1
Pyrite	3	4	4	0	8	1	0	0	0	1	0	0	1	0	2	0	0
Fluorescing H	24	36	34	42	50	36	20	14	33	36	33	30	19	38	15	27	54
Non-fluorescing (H)	35	16	15	18	11	17	48	55	15	17	29	18	40	15	72	11	7
Total Fluorescing (H + L)	35	50	41	50	59	52	35	24	41	45	45	35	38	53	11	39	71
Non-fluorescing (H + I + M)	65	50	59	50	41	48	65	76	59	55	55	65	62	47	89	61	29
H (mmf)	67	58	52	64	67	54	69	73	51	55	65	50	69	55	77	41	61
L (mmf)	13	16	7	8	11	16	15	11	9	9	13	6	21	16	12	13	17
I (mmf)	20	27	41	28	22	30	16	16	40	36	23	44	10	29	11	47	22
Rank (R_r %)	0.26	0.34	0.31	0.3	0.27	0.25	0.32	0.33	0.26	0.27	0.25	0.28	0.27	0.26	0.27	0.26	0.25
GI	2.81	1.77	0.21	1.59	0.54	1.22	2.79	2.23	0.89	0.84	3.05	0.92	4.85	1.14	2.26	0.65	2.24
TPI	0.23	1.45	0.12	1.42	0.5	0.42	1.26	0.44	0.62	0.44	0.28	0.49	0.3	0.37	1.84	0.72	0.19
GWI	5.24	0.71	0.38	0.44	0.45	1.1	0.85	1.34	0.56	0.76	5.69	1.21	3.7	1.09	0.38	0.46	6.02
VI	0.5	1.46	0.47	1.72	0.7	0.7	1.31	0.61	0.94	0.88	0.53	0.85	0.44	0.67	1.87	1.21	0.46

Min. = Minimum; Max. = Maximum; Avg. = Average; St. Dev. = Standrad Deviation

about 20–26.90 m thick at different depths (38–148 m). The overall thickness of the studied sequence is approx. 21 m, which consists of a composite lignite seam of approx. 18 m thick. The lignite seam is overlained by grey shales of variable thicknesses. The lignites are compact, sparingly banded, amorphous textured and blackish-brown in colour, and contain high in-situ moisture. The average ash yield is 11.9 wt.%, volatile matter yield is 31.81 wt.%, fixed carbon is 21.28 wt.%, and calorific value at 45% in-situ moisture is 2867 k cal./kg (GSI, 2011 unpublished Report).

3. Material and methods

The representative 43 samples were taken after removing the weathered surface (altered sediments) vertically in ascending order (channel sampling). The petrographical analysis was performed on 31 samples, while the palynological and palynofacies studies were carried out on 43 samples. The six representative samples (4 lignites, 2 shales) were subjected to GC-MS analysis for assessing the biomarkers, whereas the Rock-Eval analysis was made on 13 samples (8 lignites, 5 shales). The lithology and samples position are shown in Fig. 3.

3.1. Petrography

The sample preparation, macerals analyses (composition), and measurements of huminite (ulminite) reflectance (R_r) on crushed sample fragments (1 mm) were performed according to the ISO 7404-2, 7404-3 and 7404-5 (ISO, 2009) norms and ICCP nomenclature (ICCP, 2001; Sýkorová et al., 2005; Pickel et al., 2017). The methodology/procedure for petrographical analyses provided by Singh et al. (2017a, b, c) was followed.

3.2. Palynology

The maceration technique given by Traverse (1988) for the palynological investigation, was followed. Briefly, the crushed samples were undergone to various acid (HCl, HF, and HNO_3) subsequent treatments. The acid-free sieved samples are also treated with a 10% KOH solution for the recovery of clean palynomorphs. The Leica DM 3000 microscope

G − 18	G − 19	G − 20	G − 21	G − 22	G − 23	G − 24	G − 25	G − 26	G − 27	G − 28	G − 29	G − 30	G − 31	Min.	Max.	Avg.	St.Dev.
Macerals																	
85	74	50	77	75	58	24	41	58	66	56	79	56	79	24	85	59	13.2
31	36	31	30	35	18	13	11	20	35	34	57	45	56	**5**	**57**	**26**	**13.6**
1	2	1	0	0	0	0	0	0	0	0	3	0	1	**0**	**3**		
30	34	30	30	35	18	13	11	20	35	34	54	45	55	**5**	**55**		
28	36	15	47	37	39	10	29	39	30	19	23	9	23	**9**	**55**	**31**	**12.7**
19	4	6	3	5	1	2	6	3	1	7	4	2	15	**0**	**34**		
10	32	9	44	32	38	8	24	36	29	12	19	7	8	**7**	**55**		
26	2	4	0	3	1	1	1	0	1	4	0	2	0	**0**	**26**	**2**	**4.6**
26	2	4	0	3	1	1	1	0	1	4	0	2	0	**0**	**26**		
2	**10**	**14**	**17**	**10**	**36**	**12**	**27**	**9**	**10**	**7**	**2**	**9**	**6**	**2**	**36**	**12**	**6.7**
1	2	2	0	2	2	1	6	2	2	1	1	3	0	**0**	**6**		
0	1	3	0	1	0	1	4	0	1	1	0	1	0	**0**	**5**		
0	0	0	0	0	0	0	0	0	0	0	0	0	0	**0**	**1**		
0	3	4	3	1	3	4	10	3	3	2	1	4	1	**0**	**11**		
0	3	0	5	0	18	0	0	0	0	0	0	0	0	**0**	**18**		
0	0	0	0	0	0	0	0	0	0	0	0	0	0	**0**	**3**		
1	1	4	9	6	13	6	8	5	4	2	0	2	4	**0**	**13**		
4	**11**	**33**	**5**	**11**	**4**	**62**	**20**	**21**	**18**	**33**	**14**	**33**	**7**	**4**	**62**	**23**	**13.7**
3	8	11	3	5	0	25	6	6	8	18	2	14	1	**0**	**25**		
0	1	1	0	1	1	0	0	5	2	1	4	2	2	**0**	**8**		
1	0	4	1	2	2	2	3	0	4	1	3	4	3	**0**	**9**		
0	2	17	2	3	1	34	12	9	4	14	6	13	0	**0**	**34**		
9	**6**	**4**	**1**	**5**	**2**	**3**	**12**	**12**	**7**	**4**	**5**	**3**	**9**	**1**	**14**	**6**	**3.5**
6	3	4	1	5	2	3	10	3	3	4	5	3	6	**1**	**13**		
3	3	0	0	0	0	0	3	9	3	0	0	0	3	**0**	**9**		
8	18	35	35	49	19	21	25	30	9	38	13	36	7	**7**	**54**		
77	57	15	41	26	39	2	16	28	57	18	66	19	73	**2**	**77**		
10	27	49	52	58	55	33	51	39	18	45	15	45	12	**10**	**71**		
90	73	51	48	42	45	67	49	61	82	55	85	55	88	**29**	**90**		
93	79	52	77	79	59	24	47	66	70	58	83	58	87	**24**	**93**		
2	10	14	17	10	37	12	30	11	10	7	2	9	6	**2**	**37**		
4	11	34	5	11	4	64	23	23	19	35	15	34	7	**4**	**64**		
0.27	0.26	0.26	0.26	0.29	0.29	0.33	0.36	0.24	0.29	0.28	0.29	0.25	0.29	**0.24**	**0.36**	**0.28**	**0.0**
2.77	4.23	1.13	9.12	4.45	11.69	0.34	1.36	2.41	3.41	1.24	3.55	1.59	2.71	**0.21**	**11.69**	**2.58**	**2.4**
2	1.03	1.15	0.6	0.93	0.51	0.31	0.29	0.52	1.08	1.2	2.13	2.31	2.52	**0.12**	**2.52**	**0.89**	**0.7**
0.88	1	0.5	1.41	1.01	2.11	0.77	2.23	2.14	1.05	0.49	0.39	0.26	0.23	**0.23**	**6.02**	**1.45**	**1.6**
1.21	1.21	1.46	0.55	0.94	0.34	0.86	0.72	0.66	1.27	1.68	2.27	2.99	2.2	**0.34**	**2.99**	**1.09**	**0.6**

has been used for identification and counting (150–200 counts per sample) of the palynomorphs.

3.3. Palynofacies

The procedure for the palynofacies (sedimentary organic matter) study has been provided by Batten (1996) and Batten and Stead (2005). As per the classification of Mendonça Filho et al. (2010, 2011, 2012), the calculation of the OM was made, under the optical microscope with transmitted light. The detailed procedure provided by Singh et al. (2017a, b, c), has been followed.

3.4. Organic geochemistry (Gas Chromatography-Mass Spectrometry)

For assessing the biomarker composition, the oven-dried powdered samples were first treated with the solution of dichloromethane: methanol (9:1), to obtain the soluble organic matter by ultrasonication for 30 min. The soluble (saturated and aromatic) fraction was analyzed on a gas chromatograph (Agilent 7890A) connected with a mass spectrometer (Agilent 5975C). The detailed methodology is given in Singh et al. (2017a, b, c) has been followed.

3.5. Rock-Eval pyrolysis

The method is useful in the quick assessment of the kerogens (types), thermal maturation (T_{max}) and the hydrocarbon potential (S1 and S2). The 'Turbo' Rock-Eval-6 Pyrolyser, used for the analysis of representative samples. The procedure of Rock-Eval suggested by Espitalié et al. (1977) and Lafargue et al. (1998) have been followed.

4. Results

4.1. Maceral and mineral constituents

The petrographical constituents and the frequency distribution of the samples (lignite) are enumerated in Table 1. The vertical distribution frequency of maceral groups and various petrographic indices has been shown in Fig. 4. The photomicrographs (in both white and fluorescence

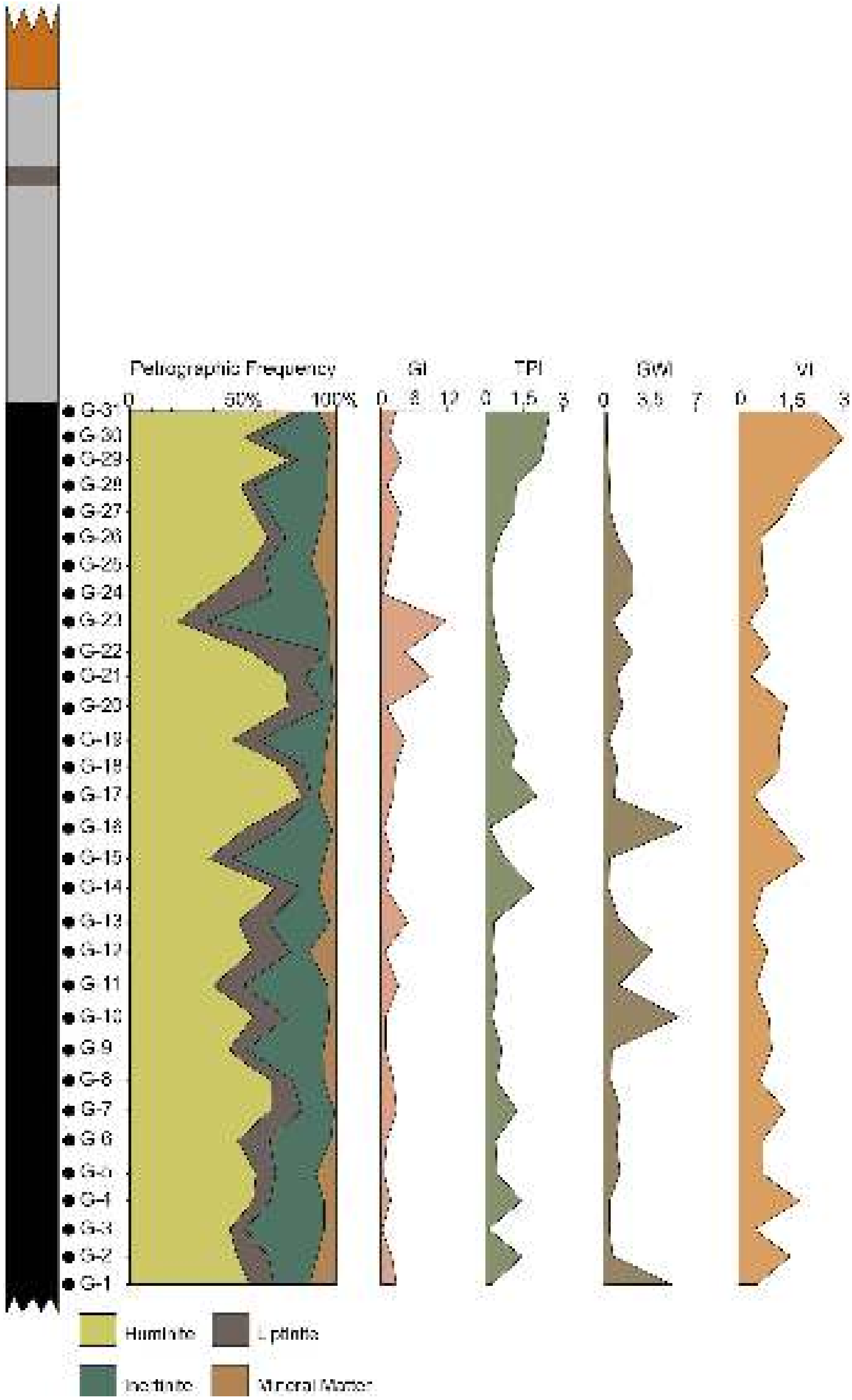

Fig. 4. Frequency distribution of various maceral group and petrographical indices of the studies lignites.

light mode), showing the different maceral types and association of various macerals are furnished in Fig. 5.

The results show huminite as the dominant maceral group (24–85 vol.%, av. 59 vol.%) in the lignites, and is mainly represented by detro-huminite sub-group (av. 31 vol.%) constituting detrital macerals–attrinite and densinite. The structured telohuminite, incorporating ulminite and textinite, is the subdominant sub-group (av. 26 vol.%), followed by the gelohuminite sub-group of macerals represented only by the corpohuminite maceral (av. 2 vol.%). The perhydrous/fluorescing huminites are found to be high in most of the samples.

The inertinite in lignites is a subdominant maceral group ranging of 4–45 vol.% (barring one high value: 62 vol.%, av. 23 vol.%) of the

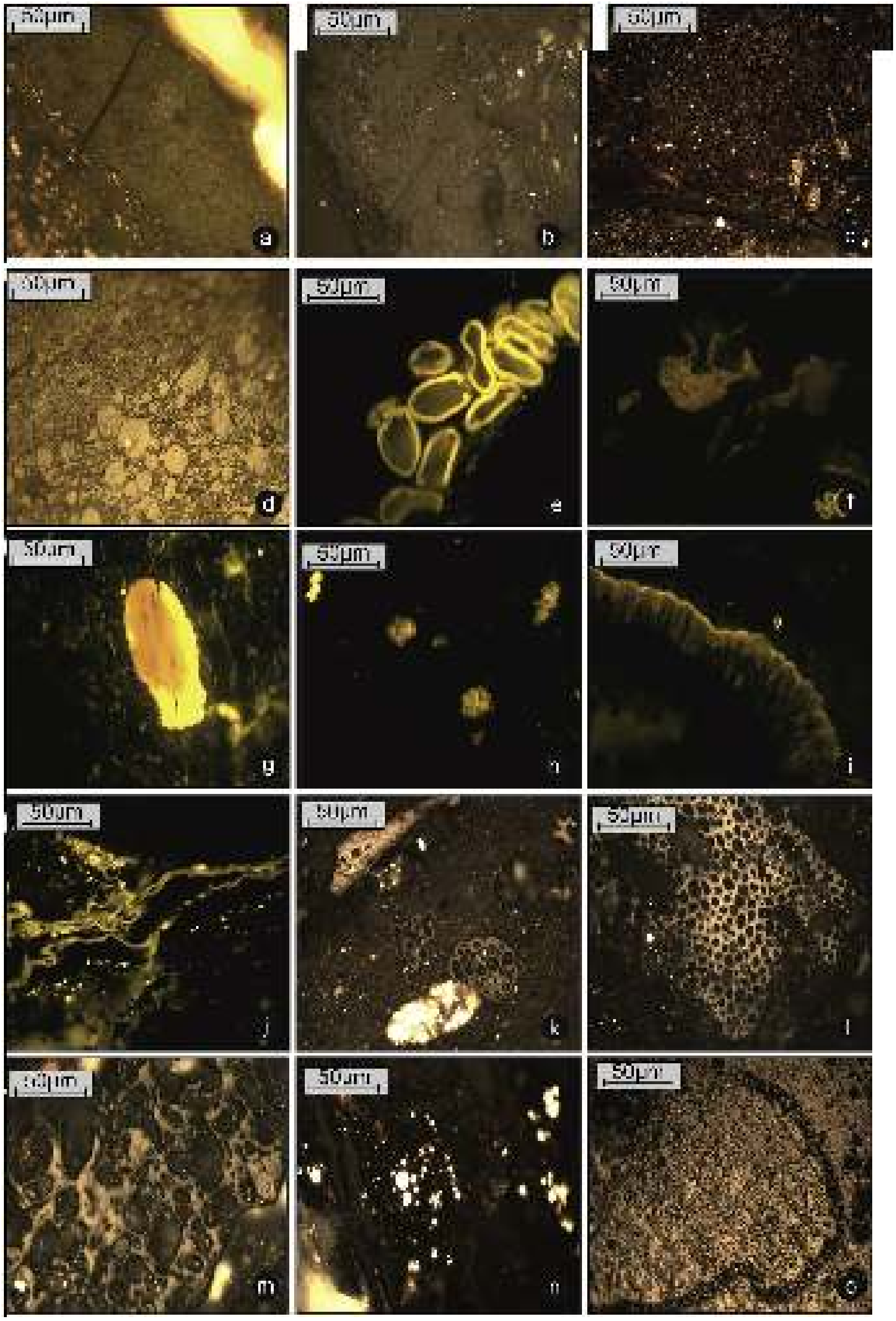

Fig. 5. Representative photomicrographs of macerals of Gurha lignite, (a) ulminite, (b) textinite, (c) detrinite, (d) corpohuminite, (e,f) sporinite (cluster), (g) resinite, (h) alginite, (i) cutinite, (j) sporinite (megaspore), (k) funginite, (l–m) semifusinite, (n–o) pyrite. Photomicrographs were taken under reflected white light (a–d, k–o) and in fluorescence mode (e–j).

maceral composition. It is represented by the inertodetrinite (av. 10 vol.%), semifusinite (av. 9 vol.%), funginite (av. 3 vol.%) and fusinite (av. 2 vol.%) macerals in order of abundance. The broken/fine fragments of all the macerals of this group are documented as inertodetrinite. A few studied samples also exhibit a transformation of huminite into semifusinite. The single to multi-chambered fungal spores of funginite appears as oval/elliptical bodies. The liptinite group is mainly represented by the liptodetrinite, resinite (resin/wax, etc.), sporinite (spore/pollens), and cutinite macerals, and constitutes an average of 12 vol.%, making it the least abundant group. However, sample No. 23 is enriched with alginite maceral (18 vol.%), in particular.

The mineral matter contents in the studied lignites are varying between 1 vol.% and 13 vol.% (av. 6 vol.%), mainly characterized by pyrite and clay minerals. Pyrite (0–9 vol.%) occurs as both framboidal and disseminated forms. The clastic minerals are present with almost all the macerals and occurred as micro-bands, granules, and lumps.

4.2. Thermal maturation (rank)

The information about the thermal maturation of studied lignite samples has been retrieved by calculating the mean random reflectance (Rr) value on the ulminite (huminite) maceral grains. According to ISO,

Table 2
Value of reflectance and the calculated parameters (δ, V, H) of Gurha lignite samples.

S. No.	Reflectance Min.	Max.	Mean	δ (%)	V (%)	H (%)
G-1	0.2	0.31	0.26	0.08	30.38	2.36
G-2	0.27	0.4	0.34	0.09	27.42	2.52
G-3	0.24	0.4	0.3	0.11	37.86	4.28
G-4	0.24	0.37	0.29	0.09	31.7	2.91
G-5	0.22	0.32	0.26	0.07	26.78	1.89
G-6	0.2	0.29	0.25	0.06	25.98	1.65
G-7	0.26	0.46	0.32	0.14	44.75	6.33
G-8	0.24	0.39	0.33	0.11	32.14	3.41
G-9	0.2	0.32	0.25	0.08	34.01	2.89
G-10	0.23	0.31	0.27	0.06	21.35	1.21
G-11	0.22	0.3	0.25	0.06	22.95	1.3
G-12	0.23	0.35	0.27	0.08	31.14	2.64
G-13	0.23	0.29	0.26	0.04	16.19	0.69
G-14	0.2	0.31	0.26	0.08	30.3	2.36
G-15	0.23	0.31	0.26	0.06	22.05	1.25
G-16	0.22	0.29	0.26	0.05	19.33	0.96
G-17	0.2	0.3	0.23	0.07	30.59	2.16
G-18	0.24	0.3	0.26	0.04	16.1	0.68
G-19	0.2	0.3	0.25	0.07	27.78	1.96
G-20	0.21	0.3	0.25	0.06	25.56	1.63
G-21	0.2	0.32	0.26	0.08	33.08	2.81
G-22	0.22	0.36	0.29	0.1	34.74	3.44
G-23	0.23	0.34	0.28	0.08	27.86	2.17
G-24	0.26	0.41	0.32	0.11	33.02	3.5
G-25	0.24	0.47	0.35	0.16	46.47	7.56
G-26	0.21	0.3	0.24	0.06	26.29	1.67
G-27	0.24	0.35	0.28	0.08	27.62	2.15
G-28	0.24	0.35	0.27	0.08	29.02	2.26
G-29	0.24	0.38	0.29	0.1	34.42	3.41
G-30	0.2	0.28	0.24	0.06	23.14	1.31
G-31	0.22	0.36	0.28	0.1	35.05	3.47
Min.	**0.2**	**0.28**	**0.23**	**0.04**	**16.1**	**0.68**
Max.	**0.27**	**0.47**	**0.35**	**0.16**	**46.47**	**7.56**
Avg.	**0.23**	**0.34**	**0.27**	**0.08**	**29.2**	**2.54**

δ: Standard Deviation, V: coefficient of variation (V = δ × 100/Rm), H: coefficient of non-equality (H = δ2 × 100/Rm), Min.: Minimum, Max.: Maximum.

11760-2005, the calculated R_r value of 0.24%–0.36% (av. 0.28%; Table 1), indicate that these lignites are of Low-Rank B category. Hence, it may be interpreted that transformation of organic matter subjected to pre-diagenesis region, prone for gaseous hydrocarbon genesis (Taylor et al., 1998) upon maturation or with additional heating. Further, the values of random reflectance (huminite) categorized and plotted in V/II steps to illustrate the peak maturity of studied lignite to assess the hydrocarbon potential (Table 2; Fig. 6).

4.3. Palynological composition

The major recovered palynomorphs in the palynoassemblage are listed in Table 3, and some of them are represented in Fig. 7. The vertical frequency distribution of important taxa in the studied lignite-bearing sequence is furnished in Table 4 and illustrated in Fig. 8. Although few horizons are moderatley rich, generally the distribution of palynomorphs are low in the studied samples. Major palynomorphs identified belongs to the families Onagraceae, Arecaceae, Lamiaceae, Clusiaceae, Rubiaceae, Ctenolophonaceae, Lentibulariaceae, Meliaceae, Bombacaceae, Matoniaceae, Schizaeaceae, Pinaceae, Podocarpiaceae and Araucariaceae and Microthriaceae. The pollens of *Palmae* and *Triangulorites* sp. are common in most of the samples. *Triangulorites* are very rich in samples towards the upper part of the mine section (clay bed). Incidences of few Pinaceae pollens in the studied samples are of great importance.

4.4. Palynofacies composition

The assessment (identification and counting) of particulate organic matter (POM) has been performed, and the values are shown in Table 5. The vertical frequency distribution of different palynofacies constituents (Phytoclasts, AOM, and Palynomorphs) are presented in Fig. 9 and the various particulate components (photomicrographs) are shown in Fig. 10.

The analysis shows that, in general, the sediments are rich in phytoclasts (av. 61%), followed by AOM (av. 35%), and palynomorphs (av. 4%). The palynomorphs group is characterized mainly by terrestrial (spores and pollen grains) and few marine components. On the basis of evaluation of POM, three palynofacies assemblages are recognized (Fig. 9):

Palynofacies Assemblage-I is categorized by an abundance of phytoclast contents (av. 79%) with good preservation, constituting biostructure, cuticles, and fungal elements. The AOM contents are a second in abundance (av. 16%), and the palynomorphs contents (av. 5%) are less recorded. This facies observed in samples nos. G-1, G-3–17, G-20–22, G-24–26, G-28–31 and G-40.

Palynofacies Assemblage-II shows a slightly higher proportion of AOM (av. 54%) compared to phytoclasts (av. 43%). The palynomorphs are represented in a lower amount (av. 3%). The facies occur in sample nos. G-2, G-18, G-19, G-23, G-27, and G-32–35. The phytoclasts in particular non-opaque ones in the samples are represented mainly by the biostructure (av. 17%), cuticles (av. 4%) along with non-biostructure (av. 3%) and fungal filaments (av. 1%). The equant and lath shaped opaque elements are also found in appreciated frequency (av. 17%).

Palynofacies Assemblage-III is characterized by the high AOM contents (av. 83%). The phytoclasts (av. 14%) are a subordinate while, palynomorphs (av. 3%) are the least component in this facies. The facies is represented by the samples G-36–39 and G-41–43. Among phytoclasts, the opaques (av. 7%) and biostructures (av. 5%) are in relatively high proportions with fewer contents of the cuticle, non-biostructure, and fungal elements.

4.5. Biomarker constituents (Organic geochemistry)

The saturated biomarker constituent of the Gurha samples is enumerated in Table 6. The chromatograms of selected ions *m/z* 57, *m/z* 123 and *m/z* 191 showing the distribution and relative abundance of various biomarkers are presented in Figs. 11–13, respectively. Biomarkers distributions apparently indicate the organic facies and environment of deposition (Waples and Machihara, 1991; Hunt, 1996; Peters et al., 2005).

4.5.1. Normal alkanes and isoprenoids

The normal (*n*-) alkanes distribution in the studied samples vary between n-C_{14} and n-C_{35}. Both unimodal and bimodal distribution patterns are observed. A unimodal distribution suggests a high contribution from a single source. Here in lignite samples G-2, G-9, and G-31, unimodal distributions are maximizing (C_{max}) at n-C_{29}, whereas in other samples (lignite: G-15, shales: G-32 and G-41) bimodal distributions are evident with C_{max} at n-C_{17} and n-C_{29}. Bimodal distribution clearly indicates a mixed source of organic matter (Moldowan et al., 1985). Odd saturated hydrocarbons with a carbon number ranging from n-C_{15} to n-C_{25} suggest inputs from aquatic organic matter, where the lacustrine algal source is indicated by the shorter chains and macrophyte source is indicated by the longer chains (Ficken et al., 2000, 2002). The abundances of n-C_{18}, n-C_{20} is suggestive of the microbial activity (Cranwell, 1977). The high relative abundance of compounds with odd carbon number ($<C_{27}$) maximizing at n-C_{29} indicates the input of terrestrial higher plants.

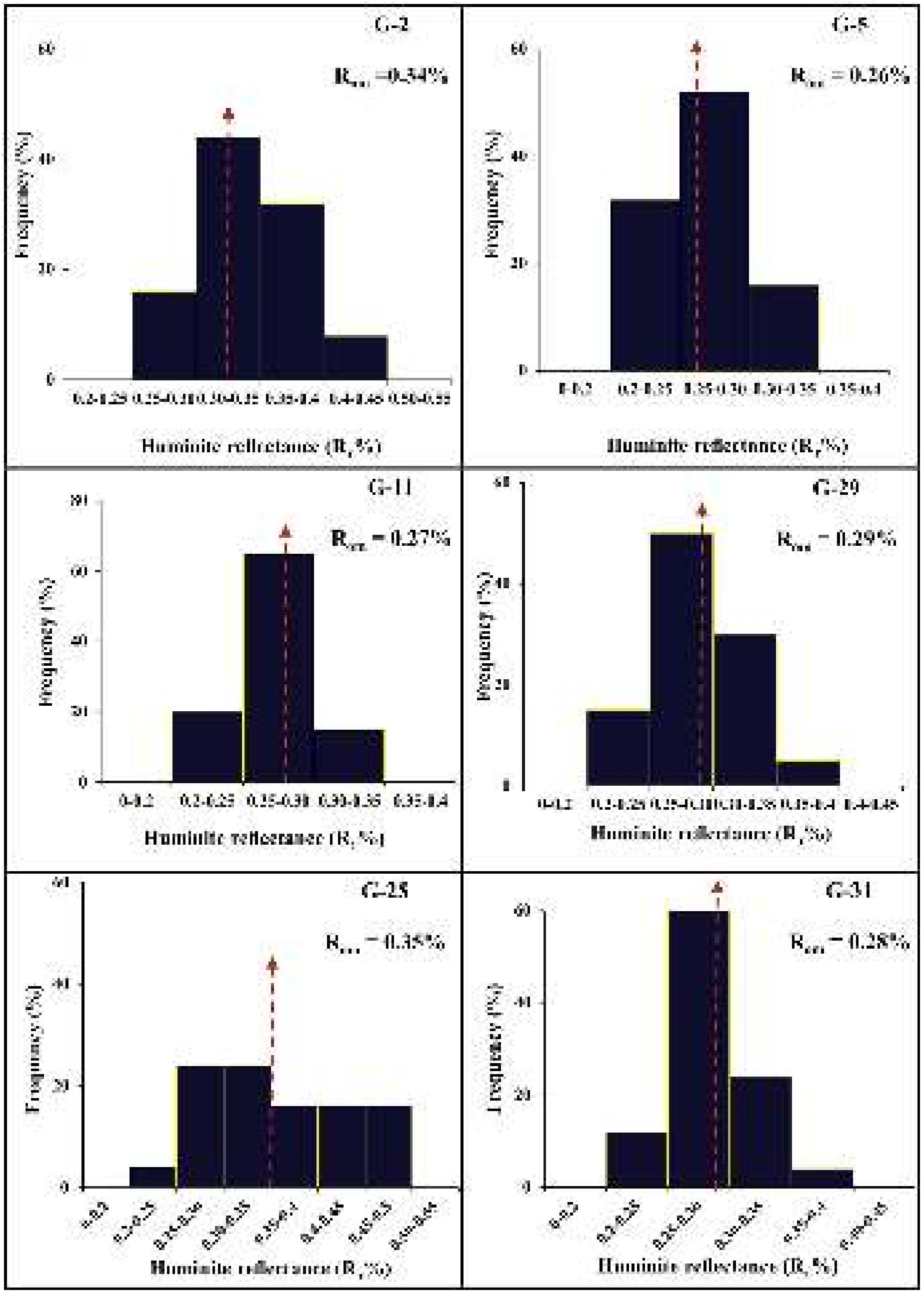

Fig. 6. V/II-step reflectograms of some representative samples of Gurha lignites.

The various *n*-alkane parameters calculated are presented in Table 7. The isoprenoid compounds pristane (Pr) and phytane (Ph) are common in all the studied samples, and the Pr/Ph ratio is greater than 1 (av. 1.9) in lignites, whereas it is less than 1 (av. 0.8) in shales. The carbon preference index (CPI; Moldowan et al., 1985) values range between 2.23 and 7.01. The terrigenous/aquatic ratio (TAR; Bourbonniere and Meyers, 1996) ranges between 2.35 and 56.20. The P_{aq} (Proxy aqueous) ranges from 0.74 to 0.94, while the P_{wax} (Proxy wax) ratios range between 0.22 and 0.58.

4.5.2. Terpenoids

The sesquiterpenoids are represented by rearranged bicyclic alkane (C_{14}), 8β (H)-drimane and 8β (H)-homodrimane. The origins of these compounds are widely unknown (Peters and Moldowan, 1993). However, according to Alexander et al. (1984) and Philp (1985), these compounds are originated from a possible hopanoid precursor via aerobic microbial activity during early diagenesis. The diterpanes are indicated by the mass chromatogram *m/z* 123 (Fig. 10). The diterpenoids found in analyzed samples include C_{18} and C_{20} diterpane, demethylated *ent*-beyerane, sandaracopimarane, pimarane, and Kaurane type of compounds.

The *m/z* 191 mass chromatogram shows C_{15} to C_{19} homologue series of tricyclic terpanes (Fig. 11). These compounds show a higher relative abundance in two samples (G-1 and G-15) of which in sample G-15, C_{15} tricyclic terpanes is the most abundant compound. The tetracyclic terpanes identified include degradation products of oleanene, ursene, and lupane. Generally, in most of the samples, hopanoids are found in abundance, but two samples (G-2, G-15) show relatively low

Table 3
Palynomorphs recorded in the lignite-bearing Gurha sedimentary sequences.

Pteridophytic spores
Monolete spores
Schizaesporites crassimurus (Mandal, 1990)
Trilete spores
Dandotiaspora dilate (Sah et al., 1971)
Dandotiasporatelonata (Sah et al., 1971)
Lygodiumsporites eocenicus (Dutta and Sah, 1970)
Lygodiumsporites pachyexinus (Saxena, 1978)
Angiosperm pollen
Monocolpate/Monosulcate
Grevilloideaepites pachyexinus (Singh and Misra, 1991)
Monosulcites major (Dutta and Sah, 1970)
Palmipollenites sp.
Proxapertites microreticulatus (Jain et al., 1973)
Polylongicolporites verrucatus sp.
Polycolporites microreticulatus sp.
Polybrevicolporites sp. (Singh et al., 1992)
Bacuspinulopollenites baculatus (Singh and Misra, 1991)
Fevitrireticolpites sp.
Retistephanocolpites multirimatus (Saxena, 1982)
Retistephanocolpites flavatus (Saxena, 1979)
Ctenolophonodites sp.
Polycolpites ornatus (Dutta and Sah, 1970)
Meliapollis pachydermis (Navale and Misra, 1979)
Lakiapolliollis ornatus (Dutta and Sah, 1970)
Lakiapolliollis ovatus (Venkatachala and Kar, 1969)
Gymnosperm Pollen
Pinuspollenites sp.
P. crestus
Araucaria sp.
Fungal fruiting bodies
Phragmothyrites eocaenica (Kar and Saxena, 1976)
Callimothallus assamicus (Kar et al., 1972)
Multicelliasporites tener (Kalgutkar and Jansonius, 2000)
Dinoflagellate cysts.

concentrations. The most abundant hopanoids are 30-norhop-17(21)-ene, Hop-17(21)-ene, 17β(H)-22,29,30-Trisnorhopane, 17β(H),21β(H)-30- ββ-hopane and Norhopane.

4.6. Rock-Eval pyrolysis and total organic carbon (TOC) analyses

The analysis suggests that the free hydrocarbon (recorded as S1 curve) contents range of 1.09–16.05 mg HC/g for the lignites, and 0.64–1.82 mg HC/g for the associated shales. The amount of hydrocarbon yield (S2), released due to the breaking of larger molecules of the OM, varies between 63.59–247.88 mg HC/g (lignites) and 16.30–214.39 mg HC/g (shales). The contents of CO_2 produced during pyrolysis (under the S3 curve) are ranges of 5.15–26.07 mg CO_2/g (Table 8).

The TOC contents is avital parameter for the measurement of the hydrocarbon generative potential (Tissot and Walte, 1984; Peters, 1986). The amount (quantity) of OM present in the sediment, generally articulated as total organic carbon; however, OM not only contains carbon but also have oxygen, nitrogen, sulphur and hydrogen. The TOC ranges of 13.03–58.76 wt.% in the studied samples (Table 8). The ranges of hydrogen index (HI) and oxygen index (OI) between 101 and 546 mg HC/g TOC, and from 31 to 91 mg CO_2/g TOC, respectively. The mineral matter contents might have some influence on the HI values, causes a low HI content (Horsfield et al., 1988; Littke et al., 1989; Jasper et al., 2009; Mendhe et al., 2017a, b; Mendhe et al., 2018a, b, c). Kotarba et al. (2002) and Varma et al. (2015) suggested that the presences of some stable oxygen moieties (not cracked immature sediments) may be attributed to low OI values. The temperature maxima (T_{max}) varies between 395 °C and 429 °C, values are uniform and are well-corroborated with the rank data of the studied lignites. The production index (PI) is also a crucial geochemical parameter for maturity if the source rock is not affected by hydrocarbon expulsion or impregnation (Jasper et al., 2009). The analyzed PI values vary between 0 and 0.1.

5. Discussion

5.1. Palaeovegetation

The Gurha lignite deposits are predominantly composed of huminite macerals (Singh et al., 2016; Singh and Kumar, 2018; Razak et al., 2019), angiosperm pollens and phytoclasts OM along with fair representation of sporinite (spores-pollen), cutinite (cuticles) and resinite (resin/wax, latex, etc.) indicating higher (angiosperm and gymnosperm) plant input. This primary input is further indicated by the high relative abundance of compounds with odd carbon number ($<C_{27}$) maximizing at n-C_{29}. Also, the occurrence of Onagraceae family pollens in great frequency points to the high input of resin-producing vegetation, occurring in a dense forest, contributes to the peat formation. The better preservation of tissues is aided by the high content of lignin in the woody materials (Oikonomopoulos et al., 2013). The tetracyclic terpanes present in the lignite extracts are primarily considered as diagenetic products of the microbial activity (Corbet et al., 1980; Jacob et al., 2007). During diagenesis, in angiosperms, the oxygenated triterpenoids compounds like α amyrin, β amyrin, and lupeol, forms these biomarker compounds (Trendel et al., 1989; ten Haven et al., 1992; Jacob et al., 2007). The presence of these compounds in Gurha deposits suggests the terrigenous (angiosperm) input into the OM.

The carbon preference index (CPI) provides general information on organic matter source, and the value ≥ 1 indicates coaly source OM (Moldowan et al., 1985). Whereas, the terrigenous/aquatic ratio (TAR) shows the relation between the terrigenous inputs and the aquatic input (Peters et al., 2005). The CPI values are ranging from 2.23 to 7.01 and TAR values ranging from 2.35 to 56.20 in the analyzed samples. The values indicate a considerably high input of terrigenous plants. The P_{wax} (Proxy wax) ratios range between 0.22 and 0.58 indicate the significant influence of the higher land plant to OM (Zheng et al., 2007). Most of the western Indian lignites are presumed to be formed from the angiosperm dominant forest vegetation (Dutta et al., 2011; Singh et al., 2013; Paul et al., 2015; Singh et al., 2015a, b, 2017a, b, c, 2018 and many others). The detrohuminites is formed by the contributions of the soft-wood plant (the herbaceous vegetation) and/or the mechanical degradation of higher plant tissues by the increased bacterial activity on the peat biomass (Diessel, 1992). The physical breakdown of the OM before deposition can also lead to the enrichment of the detrohuminite contents (Iordanidis and Geogikopoulos, 2003). In the studied samples, the appreciable amount of detrohuminiteis indicative of herbaceous input and bacterial degradation.

Further, the variation in V/II steps reflectograms (Fig. 6) suggests that the organic matter was derived from two or more sources (Hazra et al., 2015; Varma et al., 2018). Varma et al. (2018) have demonstrated the source of deposited organic matter empirically by calculating the coefficient of non-equality (H), the standard deviation (δ) and the coefficient of variability (V). The values of these parameters (H: 0.68%–7.56%; δ: 0.04%–0.16%; V: 16.10%–46.47%; Table 2), in the studied samples, also points towards the heterogeneity in the organic source material. This heterogeneity in the organic matter composition has exerted control over reactivity and could play an essential role in the hydrocarbon generation (Varma et al., 2018 and the ref. therein).

The P_{aq} (Proxy aqueous) ratio in the studied samples varies between 0.74 and 0.94, suggesting the critical contribution of submerged or floating macrophyte input in peat formation (Ficken et al., 2000). The hopanoids observed in the lignite extracts are also indicated a considerable bacterial degradation of the peat biomass. These compounds are found in aerobic bacteria, fungi, and cryptogams (Bechtel et al., 2001). Thus, the abundance of n-C_{18}, n-C_{20} and hopanoids point toward

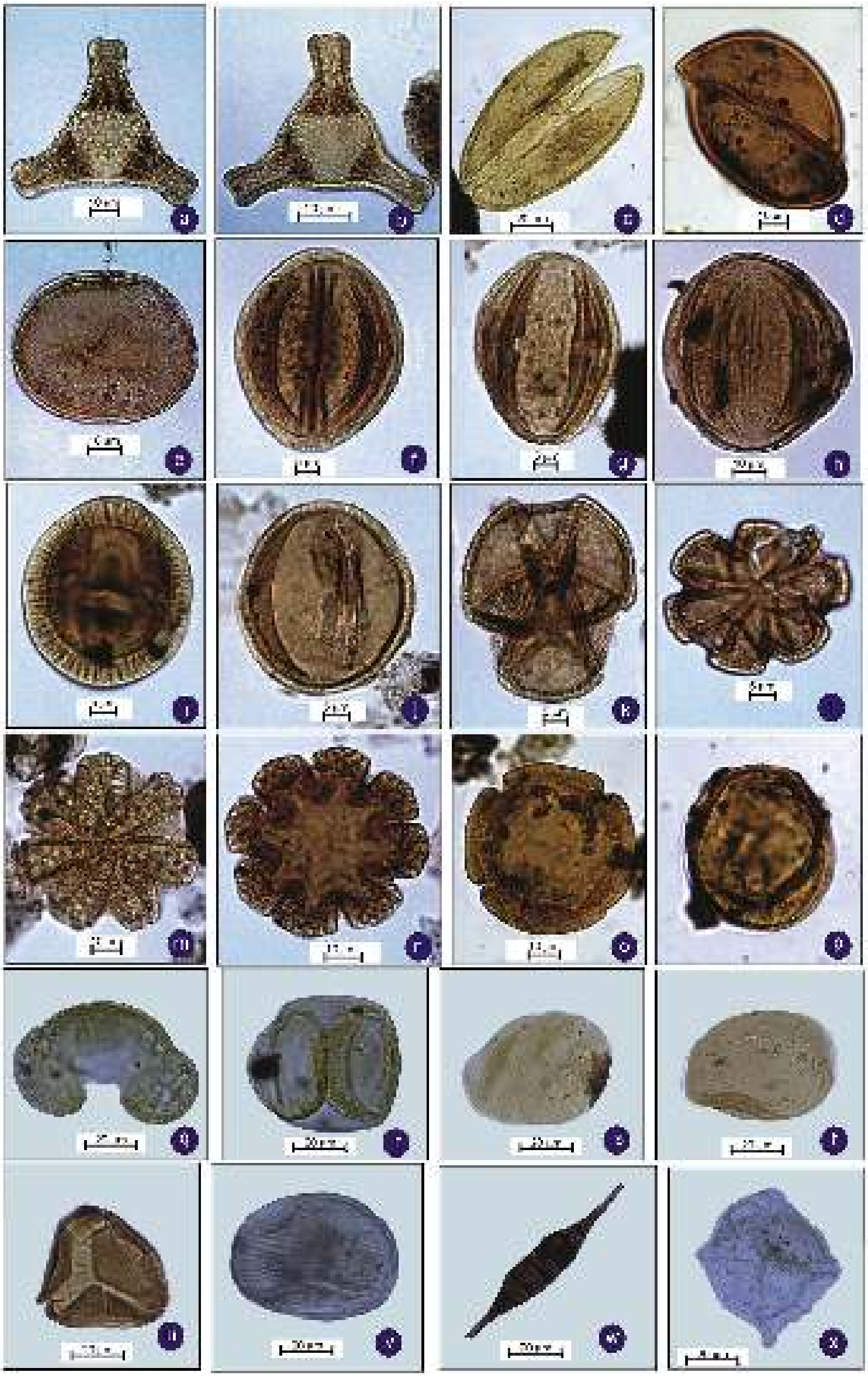

Fig. 7. Palynomorphs recovered from the studied Gurha samples: (a) *Grevilloideaepites pachyexinus*, (b) *Grevilloideaepites pachyexinus*, (c) *Monosulcites major*, (d) *Palmipollenites* sp., (e) *Proxapertites microreticulatus*, (f) *Polylongicolporites verrucatus* sp., (g) *Polycolporites verrucatus* sp., (h) *Polycolporites microreticulatus* sp., (i) *Polybrevicolporites* sp., (j) *Bacuspinulopollenites baculatus*, (k) *Fevitrireticolpites* sp., (l) *Retistephanocolpites multirimatus,* (m) *Ctenolophonodites* sp., (n) *Polycolpites ornatus*, (o) *Meliapollis pachydermis*, (p) *Lakiapollis ornatus*, (q) *Pinuspollenites crestus*, (r) *Pinuspollenites* sp., (s–t) Araucaria pollen, (u) *Dandotiaspora dilate*, (v) *Schizaeosporites crassimurus*, (w) *Multicelliasporites* sp., (x) *Dinoflagellate cyst*.

increased microbial activity. Further, the occurrence of tricyclic terpanes also suggests the microbial or algal origin (Aquino Neto et al., 1983; Azevedo et al., 1992). Along with these, inputs from the algal communities are also identified by the peaks maximizing at n-C_{17} and n-C_{19} in some samples. The presence of spores of family Rhizophoraceae in the palynoassemblage indicates mangrove-mixed source vegetation.

Further, the relatively high contents of telohuminite also point towards the higher degree of protection to bacterial degradation by resins produced by gymnosperms (Drobniak and Mastalerz, 2006) in some samples. Earlier studies show that coals/lignites originated from the conifer-forests displayed better preservation of cellular tissues than angiosperm sourced coals (Cameron et al., 1984; Teichmüller, 1989; Taylor et al., 1998). Here, although found in low frequency, the occurrence of Pinaceae family pollen is noticeable in the recovered palynoassemblage and indicates the presence of gymnosperm vegetation in the hinterland. Moreover, the organic extracts show the presence of diterpanes in Gurha mine samples. These biomarker compounds are the indicators of conifer plants and derived precisely from essential oils and resinous substance. In the extant gymnosperms, compounds with phyllocladane skeleton are characteristic of the families Cupressaceae,

Table 4
Vertical frequency distribution (in%) of recovered palynotaxa in Gurha (east) lignite mine.

Sample No.	*Grevilloideapites pachyeximus*	*Monosulcites major*	*Palmidites sp.*	*Proxaperites microreticulatus*	*Polylongicolporites verrucatus sp.*	*Polycolporites verrucatus sp.*	*Polycolporites microreticulatus sp.*	*Polybrevicolporites sp.*	*Bacuspinulopollenites baculatus*	*Fevitrireticolpites sp.*	*Retistephanocolpites multirimatus*	*Ctenolophonidites sp.*	*Polycolpites ornatus*	*Meliapollis pachydermis*	*Lakiapollis ornatus*	*Pinuspollenite screstus*	*Pinuspollenites sp.*	*Araucaria pollen*	*Araucaria pollen*	*Dandotiaspora dilate*	*Schizaeosporites crassimurus*	*Mulicelliasporites sp.*	*Dinoflagellate cyst*
G-43	0	0	0	0	0	0	0	0	0	0	0	0	0	0	0	0	0	0	0	0	0	0	0
G-42	0	0	0	0	0	0	0	0	0	0	0	0	0	0	0	0	0	0	0	0	0	0	0
G-41	0	0	0	0	0	0	0	0	0	0	0	0	0	0	0	0	0	0	0	0	0	0	0
G-40	0	0	0	0	0	0	0	0	0	0	0	0	0	0	0	0	0	0	0	0	0	0	0
G-39	0	0	0	0	0	0	0	0	0	0	0	0	0	0	0	0	0	0	0	0	0	0	0
G-38	0	0	0	0	0	0	0	0	0	0	0	0	0	2	0	0	0	0	2	0	0	0	0
G-37	0	0	0	0	0	0	0	0	0	0	1	1	0	0	2	0	0	0	2	0	0	0	0
G-36	0	0	0	0	0	0	0	0	0	0	0	0	0	0	0	1	0	0	0	0	0	0	0
G-35	0	0	0	0	0	0	2	0	0	0	0	0	0	0	3	0	0	0	0	0	0	0	0
G-34	0	0	0	0	0	0	0	0	0	0	0	0	1	0	0	0	0	0	0	4	0	0	0
G-33	0	0	0	0	0	0	2	0	0	0	0	2	0	0	0	0	0	0	0	0	0	0	0
G-32	0	1	0	0	0	0	0	0	0	0	2	0	3	0	0	7	5	0	0	0	0	0	0
G-31	0	1	0	0	3	0	0	0	0	0	0	0	0	0	0	5	3	1	0	0	0	0	0
G-30	0	0	0	0	0	0	3	0	0	0	0	0	0	2	0	0	0	3	0	0	0	0	0
G-29	0	2	0	0	0	0	5	0	0	0	0	2	0	0	0	0	2	0	0	0	0	0	0
G-28	0	0	0	0	2	0	0	2	0	0	0	0	0	0	0	0	0	0	0	0	0	0	0
G-27	0	1	0	0	0	0	0	0	0	0	0	0	0	0	0	0	0	0	0	3	0	0	0
G-26	0	1	0	0	0	0	0	0	0	0	0	0	0	0	0	0	0	0	0	0	0	0	0
G-25	0	0	0	0	0	0	5	0	0	0	0	0	0	0	0	0	0	0	0	2	3	0	0
G-24	0	0	0	0	3	4	0	2	0	1	2	0	1	0	0	0	0	0	0	0	0	0	0
G-23	4	0	2	0	0	0	3	0	0	0	1	0	0	0	0	0	0	0	0	0	0	0	0
G-22	5	0	5	0	0	0	2	0	0	1	0	0	0	0	0	0	0	0	0	0	0	0	0
G-21	0	2	3	0	2	2	0	0	0	2	0	0	0	2	0	0	0	0	0	0	0	0	0
G-20	0	0	0	0	0	0	0	0	2	0	3	1	0	0	2	0	0	0	0	0	0	0	0
G-19	0	0	0	0	0	0	3	0	0	1	0	0	0	0	2	0	0	0	0	2	0	0	0
G-18	5	0	2	2	4	5	0	2	0	0	0	0	0	0	0	1	0	0	0	0	3	0	0
G-17	3	0	0	3	0	0	0	0	2	1	1	0	2	1	0	0	0	0	0	0	0	2	0
G-16	0	0	3	0	0	5	0	1	0	0	0	2	0	0	0	0	0	0	0	0	0	0	0
G-15	0	0	1	0	8	0	0	0	1	0	3	0	0	1	0	2	0	0	0	0	0	2	0
G-14	5	0	2	5	0	0	5	0	0	1	0	0	0	0	2	0	0	0	0	0	2	0	0
G-13	0	0	0	0	0	3	0	0	0	0	0	0	0	0	0	0	0	0	0	1	0	0	0
G-12	7	0	0	0	0	5	0	0	2	0	5	0	0	3	0	0	0	0	0	0	0	2	0
G-11	0	1	3	0	7	0	0	0	0	0	0	0	0	0	0	0	0	0	0	0	0	0	0
G-10	5	0	4	5	0	2	3	0	0	2	0	0	0	1	0	0	0	0	0	0	0	0	0
G-9	6	0	0	0	0	0	0	0	0	0	4	1	0	0	0	0	0	0	0	0	0	3	0
G-8	8	0	0	0	0	0	0	0	1	0	3	0	2	0	1	0	0	0	0	0	0	0	3
G-7	0	0	2	1	6	4	0	2	0	0	0	2	0	0	0	0	0	0	0	0	0	0	2
G-6	0	1	0	6	0	3	0	0	0	0	0	2	0	0	0	0	0	0	0	0	0	0	3
G-5	0	**0**	0	0	0	4	4	1	0	1	0	0	0	0	1	0	0	0	0	0	0	0	0
G-4	0	0	0	0	0	0	0	0	2	0	0	0	0	0	0	0	0	0	0	0	0	2	0
G-3	10	0	3	5	3	2	7	0	1	0	0	0	1	0	0	0	2	0	0	0	0	0	0
G-2	0	0	0	8	5	6	0	0	1	0	0	0	0	0	2	0	3	0	0	0	0	0	0
G-1	0	0	0	0	6	4	0	0	0	0	0	0	0	1	0	0	0	0	0	0	0	0	0

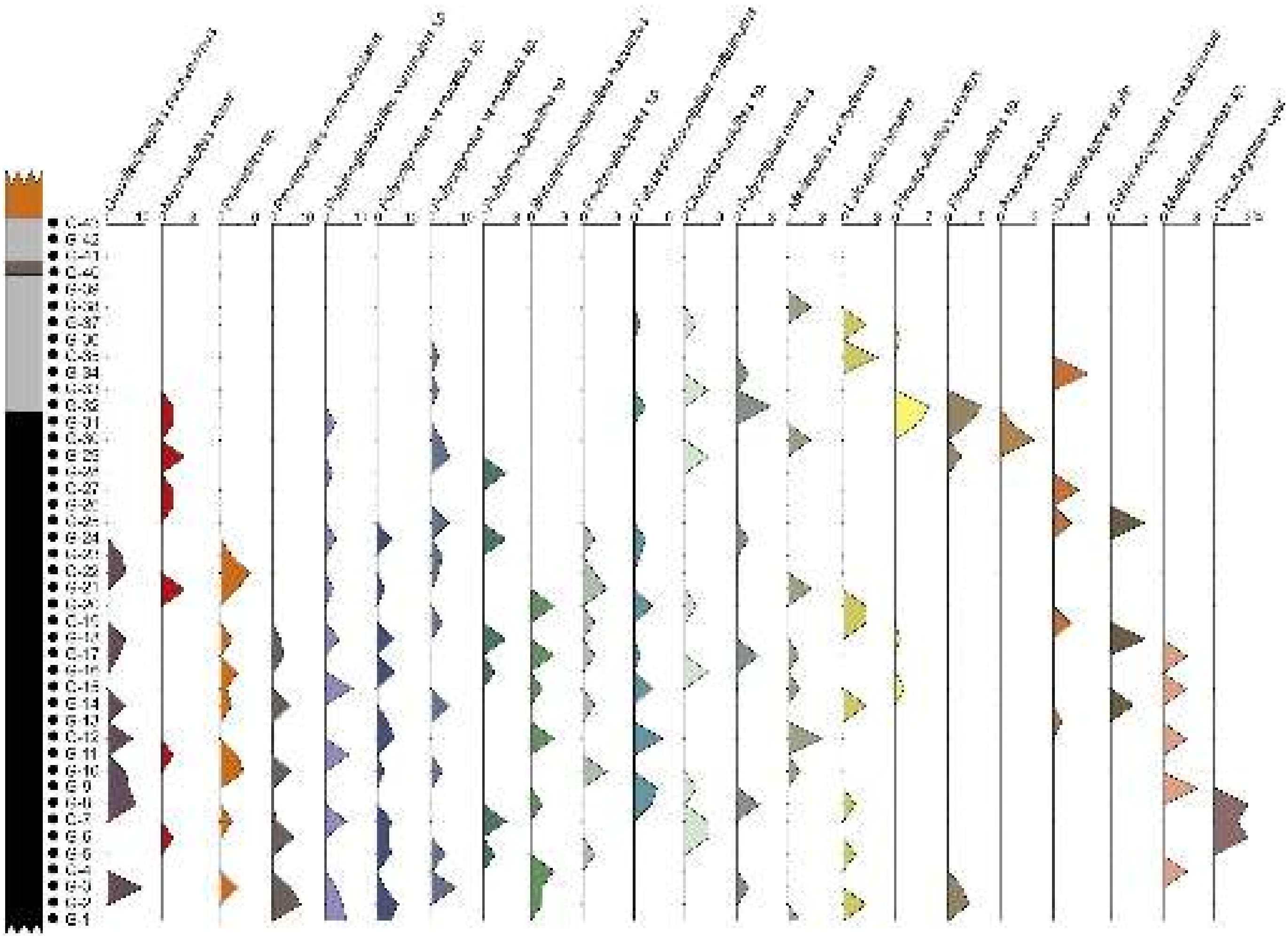

Fig. 8. Vertical distribution of different palynotaxa recovered in the studied Gurha samples.

Araucariaceae, Phyllocladaceae, Podocarpaceae, and Taxodiaceae (Karrer et al., 1977; Noble et al., 1985; Dev, 1989; Otto and Wilde, 2001). High amounts of Kauranes are often found in Araucariaceae derived oraganic matter (Stefanova et al., 2002). These types of compounds are absent in Pinaceae (Otto and Wilde, 2001; Pereira et al., 2009). However, the existence of pimarane-type diterpenoids may suggest Pinaceae, Taxodiceae and Cupressaceae source (Noble et al., 1985; Dev, 1989; Otto et al., 1997; Stefanova et al., 2002). Recently Paul and Dutta (2016) reported the existence of Araucariaceae and Podocarpaceae dominated conifers forests in western India, based on resin chemistry. In the present study also, the incidence of tetracyclic diterpenoids compounds indicate the existence of Araucariaceae and Podocarpaceae conifers forests in the Palaeocene–Eocene of Bikaner-Nagaur Basin.

5.2. Depositional palaeoenvironment

To understand the depositional patterns of the peat swamp, various organic facies indicators (TPI-GI and GWI-VI) have been utilized along with the maceral compositions (Kalkreuth et al., 1991; Silva et al., 2008, Suárez-Ruiz et al., 2012; Singh et al., 2013; Singh et al., 2017a,b, c and many others). Although these facies indicators are used widely among coal petrographers, it is recommended to be used along with other facies analysis methods such as organic geochemistry, palynology, etc. (Crosdale, 1993; Dehmer, 1995; Wüst et al., 2001; Scott, 2002; Moore and Shearer, 2003; Amijaya and Littke, 2005).

A diagram based model (Diessel, 1986) of GI and TPI indices have been estimated by using the relation given by Kalaitzidis et al. (2000) as:

$$GI = \frac{ul + gl + dn}{tx + at + in)}$$

$$TPI = \frac{(te + co + fu + sf)}{at + dn + gel + inert}$$

where, ul = ulminite; gl = gelohuminite; dn = densinite; tx = textinite, at = attrinite, in = inertinite; te = telohuminite; co = corpohuminite; fu = fusinite; sf = semifusinite; gel = gelinite and, inert = inertodetrinite.

The lignites are characterized by high GI (0.21–11.69, av. 2.58) and the moderate to low TPI (0.12–2.52, av. 0.89) values (Table 1; Fig. 5). The plotting of these values on Diessel's diagram suggests that the deposition of peat precursors was taken place in limno-telmatic to the telmatic regime (Fig. 14). The considerable variation in these values is indicating significant changes in source vegetation input as well as in bacterial degradations.

The GWI and VI relationship were given in Kalaitzidis et al. (2000), has been used to deduce the hydrological conditions and vegetation type of the palaeomire on Calder et al. (1991) facies model as under:

$$GWI = \frac{co + gel + dn + mm}{tx + ul + at}$$

Table 5
Result of palynofacies analysis of the studied Gurha samples (Mendonça Filho et al., 2012).

S. No.	Phytolasts					Total (%)	AOM (%)	Palynomorphs (%)	PF-type
	Opaque	Non-opaque							
		Cuticle	Biostr.	Non-biostr.	Fungal				
	(%)	(%)	(%)	(%)	(%)				
G-43	5.41	1	1	0.25	0	**7.66**	91.89	0.45	III
G-42	4	2	5.05	1.75	0.8	**13.6**	84.4	2	III
G-41	8.89	0	1.22	1	1.78	**12.89**	86.22	0.89	III
G-40	72.86	3	8	5.08	2.51	**91.46**	5.03	3.52	I
G-39	1.4	0	1.4	0	0	**2.8**	95.44	1.76	III
G-38	12.95	2	5	0.91	0.72	**21.58**	73.38	5.04	III
G-37	8.95	0.73	9	0	0.39	**19.07**	77.04	3.89	III
G-36	11.29	1.2	10.5	1.2	0.81	**25**	71.77	3.23	III
G-35	13.73	3	18	4.32	1.29	**40.34**	55.36	4.29	II
G-34	7.86	4	25.43	2	0.71	**40**	55	5	II
G-33	13.68	5	16	5.5	1.28	**41.46**	55.13	3.42	II
G-32	20	3	15.7	4.7	1.28	**44.68**	53.62	1.71	II
G-31	40.64	2	20.58	6.9	2.39	**72.51**	19.12	8.37	I
G-30	40.64	7.66	26.3	2	4.97	**81.57**	10.53	7.9	I
G-29	51.05	8.64	20	4	3.35	**87.03**	6.28	6.69	I
G-28	57.78	4	18	2.44	0.37	**82.59**	16.3	1.12	I
G-27	16.12	8.62	17	3	0.33	**45.07**	54.28	0.66	II
G-26	29.43	8	27.13	6	2.26	**72.83**	23.4	3.78	I
G-25	25.29	9.38	27	5	2.3	**68.97**	26.82	4.21	I
G-24	52.29	4	19	8.65	3.21	**87.15**	10.55	2.3	I
G-23	11.61	4	22	3.29	1.06	**41.95**	56.46	1.58	II
G-22	67.9	1.05	11	4	1.23	**85.19**	11.52	3.29	I
G-21	69.86	2.44	13	1	0.91	**87.22**	10.05	2.74	I
G-20	46.32	1	28.2	5	1.73	**82.25**	14.29	3.46	I
G-19	27.69	1	9.69	2	0.77	**41.15**	56.92	1.93	II
G-18	8.16	6	28.05	2	1.02	**45.23**	53.4	1.37	II
G-17	28.7	11	31.61	0	0.87	**72.18**	24.35	3.48	I
G-16	45.14	8	23	3.63	1.95	**81.71**	14.79	3.5	I
G-15	14.1	15	36	6.96	1.31	**73.36**	21.41	5.23	I
G-14	66.06	1	8	1.86	1.81	**78.73**	18.1	3.17	I
G-13	52.3	5	20.1	2.52	1.26	**81.18**	16.74	2.09	I
G-12	91.34	0	0.87	0	2.16	**94.38**	3.46	2.16	I
G-11	52.08	8.1	19	4.57	1.67	**85.42**	10.42	4.16	I
G-10	66.26	2	8.1	2.66	2.06	**81.07**	13.99	4.94	I
G-9	66.45	5	13.53	0	0	**84.98**	13.1	1.92	I
G-8	41.15	6	20.5	0.53	1.91	**70.09**	24.64	5.27	I
G-7	32.29	2	12	3.94	1.79	**52.02**	32.29	15.69	I
G-6	51.32	4	12.1	4.29	2.3	**74.01**	17.43	8.56	I
G-5	58.1	6.99	18	1	0.92	**85.01**	13.15	1.84	I
G-4	51.61	2	16	7.35	8.76	**85.72**	6.91	7.37	I
G-3	62.87	1	9	3	2.05	**77.91**	19.75	2.34	I
G-2	39.83	2	6.5	0.51	0.84	**49.68**	48.64	1.68	II
G-1	49.17	4.35	17	2	1.65	**74.18**	21.28	4.54	I
Min.	**1.4**	**0**	**0.87**	**0**	**0**	**2.8**	**3.46**	**0.45**	
Max.	**91.34**	**15**	**36**	**8.65**	**8.76**	**94.38**	**95.44**	**15.69**	
Avg.	**37.08**	**4.1**	**15.69**	**2.95**	**1.65**	**61.46**	**34.76**	**3.78**	

$$\mathrm{VI} = \frac{(\mathrm{te} + \mathrm{su} + \mathrm{re} + \mathrm{sf} + \mathrm{fu})}{\mathrm{detro} + \mathrm{inert} + \mathrm{cu} + \mathrm{sp} + \mathrm{al} + \mathrm{bi} + \mathrm{lipto}}$$

where, co = corpohuminite; gel = gelinite; dn = densinite; mm = mineral matter; tx = textinite; ul = ulminite; at = attrinite; te = telohuminite; su = suberinite; re = resinite; sf = semifusinite; fu = fusinite; detro = detrohuminite; inert = inertodetrinite; cu = cutinite; sp = sporinite; al = alginite; bi = bituminite; lipto = liptodetrinite.

The GWI values of the Gurha lignites range from 0.23 to 6.02, and the VI values fluctuate from 0.34 to 2.99 (Table 1; Fig. 5), suggesting that the basin in general witnessed varying mesotrophic to rheotrophic hydrological conditions (Fig. 15). However, few samples also show ombrotrophic condition, suggesting sporadic aerial exposure of peat surface. During exposed conditions, the oxidation of humic substances leads to the formation of inertinite macerals (Diessel, 1992; Sýkorová et al., 2005). Simultaneously, hopanoid compounds degrade to form sesquiterpenoid compounds such as rearranged bicyclic alkane (C_{14}), 8β(H)-drimane and 8β(H)-homodrimane (Alexander et al., 1984; Weston et al., 1989). Hence, the intermittent ombrotropic conditions in the mire are also evidenced by the moderatley high inetrinite contents and the presence of the aforementioned sesquiterpenoid compounds in some samples.

The extrapolation of palynofacies composition of samples on the APP (amorphous OM-phytoclasts-palynomorphs) ternary diagram of Tyson (1995) characterizes by three palyno-fields: (1) marginal dysoxic-anoxic basin (II); (2) proximal suboxic-anoxic shelf (VI) and (3) distal-suboxic-anoxic basin (IX) fields (Fig. 16).

The marginal dysoxic-anoxic basin field (II, palynofacies Assemblage-I) is dominated by opaque phytoclast along with biostructured and cuticle components of non-opaque phytoclasts, indicating the presence of dense arborescent vegetation in the vicinity of the depositional site. The relatively high phytoclasts in this facies together with the low AOM

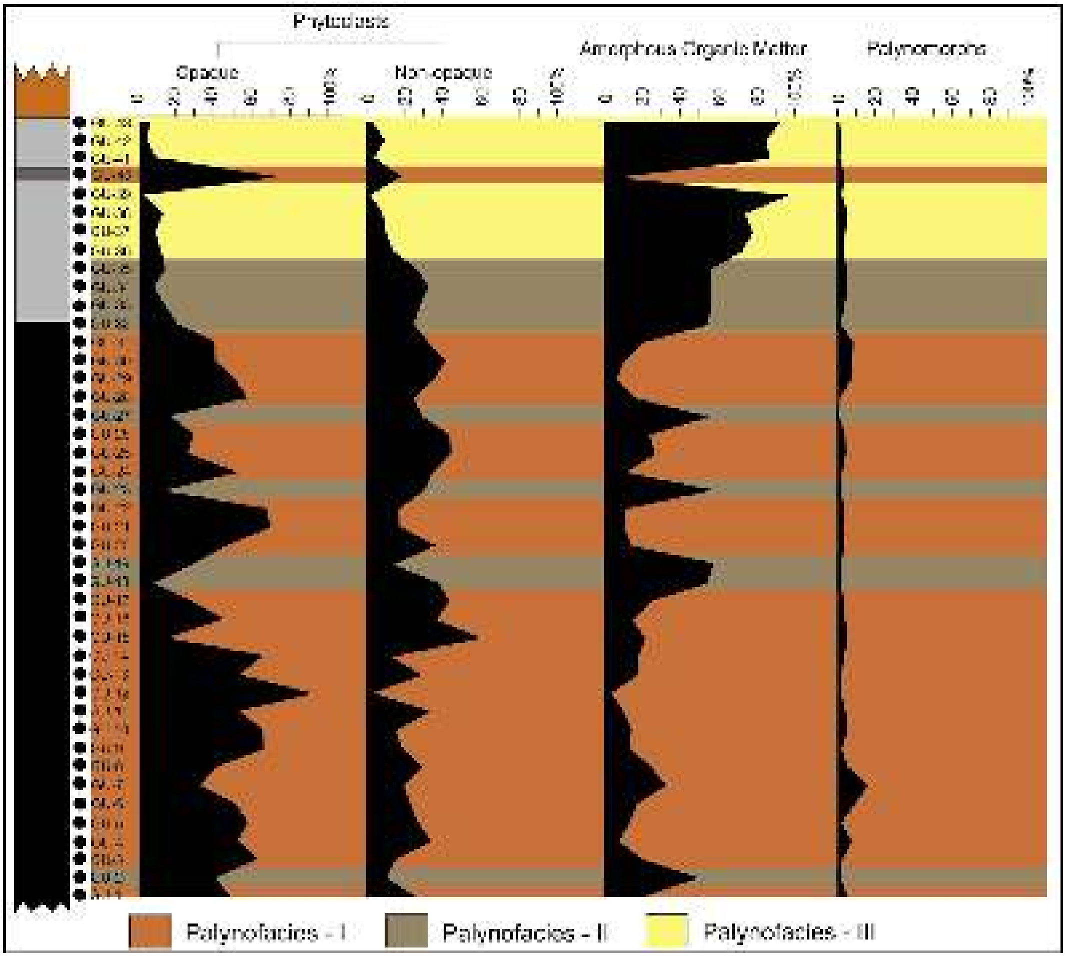

Fig. 9. Vertical distribution of palynofacies components and facies identified in the studied Gurha succession.

contents, also suggestive of an enhanced terrigenous input accumulated in anoxic condition under the proximal setting. The exceeding concentration of opaque phytoclasts over the non opaques commonly associated with high energy environments and more oxic conditions (Smyth et al., 1992; Carvalho et al., 2013). Further, the occurrence of non-biostructured phytoclasts (although in low concentration) also indicates that the OM could have undergone some (pre- and post-depositional) alterations. Therefore, a moderately high energy environment and dysoxic-anoxic conditions can be attributed to palynofacies Assemblage-I.

The proximal suboxic-anoxic shelf (VI, palynofacies Assemblage-II) is characterized by the high incidence of phytoclasts with the relatively high amount of AOM and indicate that during deposition an O_2-deprived zone was formed near to the fluvio-deltaic sources (Tyson, 1995). The occurrence of significant contents of AOM in the proximal setting could be due to the enhancement of water column in the proximal setting, leading to the formation of low-oxygen zone/environment, this reducing (low-oxygen) zone/environment is ideal for AOM preservation. It is also noted that the high AOM contents are generally associated with dysoxic conditions and/or with the sediments usually accumulated by upwelling water (Summerhayes, 1983 and the references therein). Therefore, from this facies, a suboxic-anoxic condition associated with shoreline and brackish/freshwater environment can be inferred.

Distal-suboxic-anoxic basin (IX, palynofacies Assemblage-III) represents the overall dominance of well-preserved AOM. The AOM contents are reported to have increased towards the basin direction in suboxic-anoxic conditions (Dow and Pearson, 1975; Bujak et al., 1977). Similarly, a low frequency of phytoclasts, constituting woody tissues, bio-structured and fungal remains in this facies indicates remoteness with the fluvial channel; suggestive of the suboxic conditions. The occurrence of fungal elements (although low) indicate a warm and humid environmental condition, these elements (bodies) infested the phytoclast and destroy their cellular structure, thus decreasing the frequency of well-preserved phytoclasts (Peters et al., 2013). The palynomorphs are represented by terrestrial and marine elements indicating intermixing of flora and the marine incursion at the termination point of peat accumulation in distal settings.

The land derived spores-pollen recovered in palynological assemblage suggests that the floristic association was tropical to sub-tropical and controlled by humid climatic condition during the deposition of lignite-bearing Palana Formation (Table 9). Further, the presence of *Uvaria palaeozeylanica* (leaf) reported by Shukla and Mehrotra (2014), *Aporosa ecocenicus* (leaf), *Leguminocarpon cajanoides* (fruit), and *Leguminocarpon saracoides* (fruit) by Shukla and Mehrotra (2016), *Dioscorea* (Mehrotra and Shukla, 2019) from Bikaner-Nagaur Basin also suggests the existence of mixed (tropical evergreen/semi-arid/rainforest) environmental condition (Shukla and Mehrotra, 2018; Mehrotra and Shukla, 2019) in and/or around the mine area. The palynoassemblage consists mainly of the lowland plants (angiosperms), and cosmopolitan group of plants (pteridophytes) and few gymnospermous pollen grains (*Pinus*,

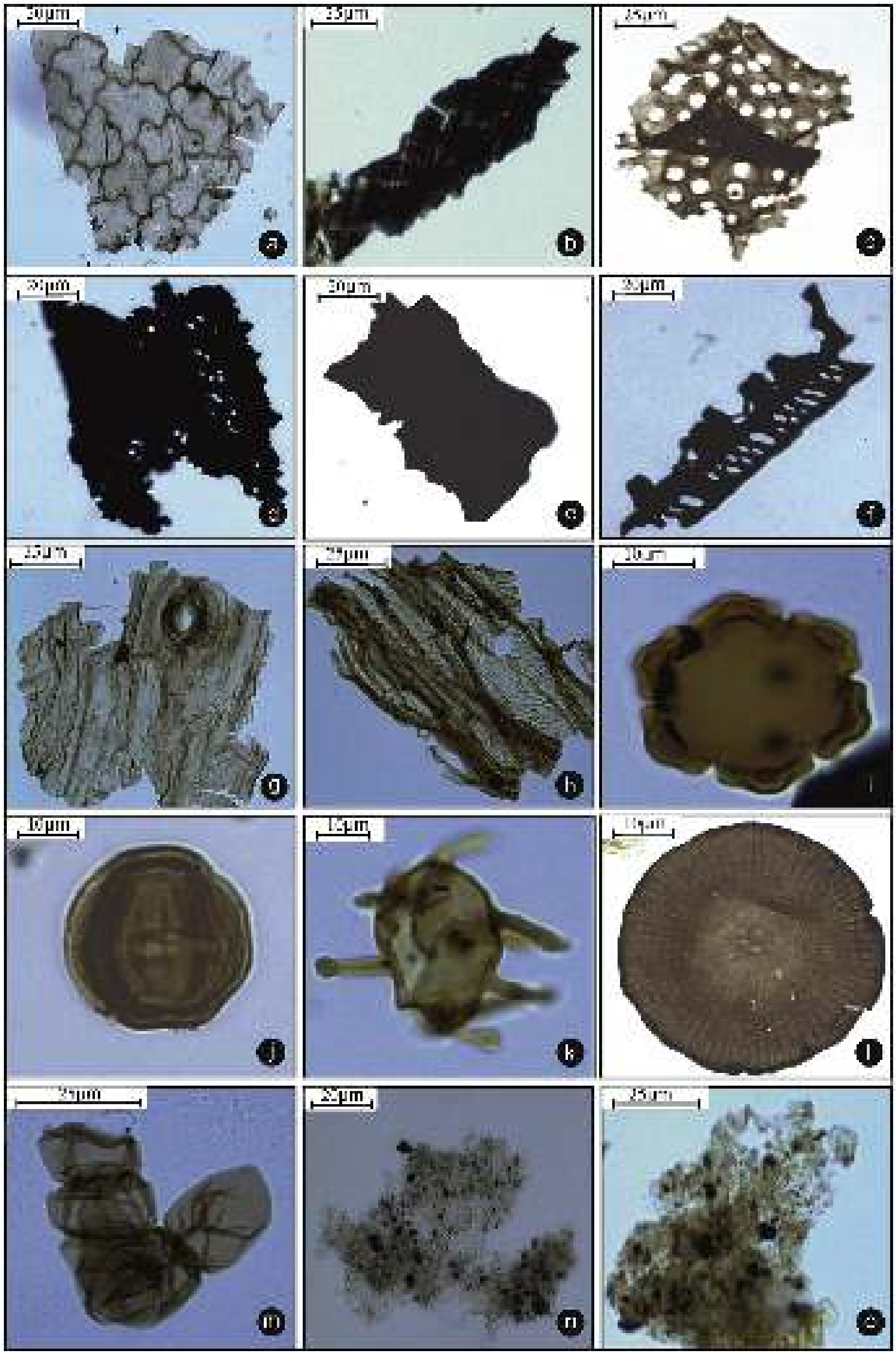

Fig. 10. Representative photomicrographs of palynofacies components, (a–b) cuticle, (c–d) biostructure phytoclast, (e) non-biostructure phytoclast, (f–h) opaque phytoclasts, (i–k) palynomorphs, (l–m) fungal elements, (n–o) amorphous organic matter.

Abies, Podocarpus). The rich preservation of angiosperm pollen shows a dense and lowland forest. Shukla et al. (2014) also reported (from Gurha mine) the occurrence of Gunnera, an uncommon tropical feature, suggest that the conditions were probably more temperate (cooler) than in present equatorial regions (Kumar et al., 2016). The presence of gymnospermous pollen suggests that either they might have transported from the surrounding hilly areas of temperate zones, or a mix of lowland flora and highland flora thriving in close environments. The varieties of palynomorphs found are assigned to various ecological groups of plants such as mixed deciduous moist forest, freshwater swamp, and mangroves. These forms indicate tropical-subtropical to a warm temperate climate with evergreen to the semi-evergreen mixed forest environment. The copious funginite maceral also supports warm and moist conditions during the biomass deposition. The occurrence of framboidal pyrite in lignites and the presence of marine dinoflagellate cysts including with coastal evidence of arecaceous pollen grains (*Monosulcites major*, *Palmidites* sp., *Proxapertites microreticulatus*, *Spinizonocolpite* sp., etc.) indicate marine incursion(s) during the peat development.

Table 6
Biomarker compounds identified in Gurha samples.

Peak No.	Compound	Base peak	Mol. Wt.
Sesquiterpane			
a1	Rearranged bicyclic alkane (C_{14})	179	194
a2	8β(H)-Drimane	123	208
a3	8β(H)-Homodrimane	123	222
Tricyclic terpane			
1	C15 tricyclic terpane	191	206
2	C16 tricyclic terpane	191	220
3	C18 tricyclic terpane	191	248
4	C19 tricyclic terpane	191	262
Tetracyclic terpane			
5	De-A-olean-13(18)-ene	189	328
6	De-A-Lupane	123	330
7	De-A-urs-13(18)-ene ?	313	328
8	De-A-olean-12-ene	203	328
9	17,21-secohopane (C_{26})	191	358
Diterpane			
d1	C18 Diterpane	135	248
d2	unidentified diterpane	259	274
d3	Demethylated ent-beyerane?	109	260
d4	Sandaracopimarane	245	260
d5	C20 Diterpane/Abietane	163	276
d6	ent-beyerane	123	274
d7	Pimarane	247	276
d8	Demethylated ent-beyerane?	109	260
d9	16α(H)-phyllocladane	123	274
d10	16α(H)-phyllocladane	123	274
Pentacyclic triterpanes			
10	17α(H),18α(H),21β(H)-28,30-Bisnorhopane	191	384
11	17α(H), 21β(H)-25-Norhopane	191	398
12	22,29,30-Trisnorhop-13(18)-ene	191	368
13	17β(H)-22,29,30-Trisnorhopane (Tm)	149	370
14	28,30-Bisnorhop-13(18)-ene	191	382
15	30-norhopane	191	398
16	30-norhop-17(21)-ene	191	396
17	Hop-21-ene	69	410
18	Hop-17(21)-ene	367	410
19	Neohop-13(18)-ene	191	410
20	17β(H),21β(H)-30-Norhopane	177	398
21	17α(H),21β(H)-Homohopane (22 S/R ?)	191	426
22	β,β-hopane	191	412
23	17β(H),21β(H)-Homohopane	205	426
24	17β(H),21β(H)-30,31-Bishomohopane	219	440

The pattern of *n*-alkane distribution useful in depicting the depositional settings/conditions (Waples and Machihara, 1991; Peters et al., 2005). In the lower part of the seam section (G-2, G-9) and the upper part (G-31), the relatively high terrestrial higher plant input is recoded indicating the terrigenous condition of the basin with minimum moisture conditions. Microbial activity is also persistent during the deposition of these samples. However, during the formation of shales (G-32, G-41) and the middle part of the lignite seam (G-15), higher abundance of n-C_{17} and n-C_{19} is observed indicating algal input. Although terrestrial plants and bacteria produce this compound, the aquatic alga is a significant source (Giger et al., 1980; Cranwell et al., 1987). Therefore, the copious occurrence of these compounds also suggests aquatic conditions. Pristane (Pr) and phytane (Ph) are the most common isoprenoids in the aliphatic fraction of OM extracts. The ratio between them is used to indicate the redox conditions prevailed during the deposition time (Didyk et al., 1978; Kotarba et al., 2002). Clayton (1993) suggested that OM derived from the humic coaly source usually have a high Pr/Ph ratio. The values > 3 suggest a higher plant input, deposited in oxic condition, values between 1 and 3 suggest moderate environment, and the values less than 0.8 indicate an anoxic condition (Powell, 1988). In Gurha samples, the Pr/Ph ratio is greater than 1 in lignites indicates moderate redox (oxidizing) conditions, whereas less than 1 in shales indicates reducing conditions. The Pr/n-C_{17} *vs.* Ph/n-C_{18} plot (Fig. 17) shows that the deposition took place in a terrestrial to marginal marine depositional settings.

5.3. Hydrocarbon source potential

The results of Rock-Eval pyrolysis analysis, are widely used to assess the hydrocarbon source potentials and to evaluate the thermal maturation of organic-rich deposits with an excellent degree of accuracy (Peters, 1986; Peters and Cassa, 1994; Lafargue et al., 1998; Garcia-Vallés et al., 2000; Skyes and Snowdown, 2002; Singh et al., 2017a, b; Mendhe et al., 2018a, b, c). In the studied samples, TOC contents (13.03–58.76 wt.%, av. 40.19 wt.%) are clearly above the threshold value (i.e., 0.5 wt.%). However, TOC may also include inert carbon which is having no hydrocarbon generation potential (Peters and Cassa, 1994; Mendhe et al., 2018a, b). Hence, the S2 content has more reliability to show the source-potential of a rock/sediment (Peters, 1986; Bordenave, 1993; Kumar et al., 2018).

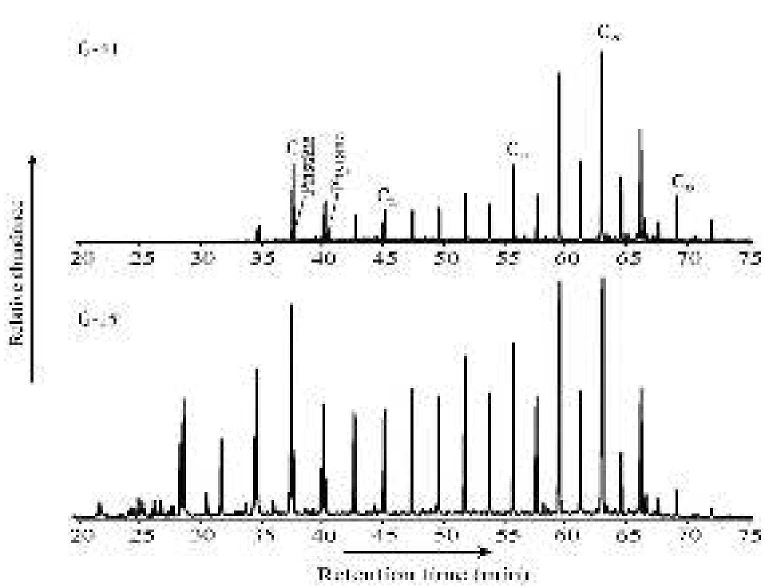

Fig. 11. *n*-alkane distribution according to SIM *m/z* 57 the studied Gurha lignite samples. Numbers correspond to carbons in the *n*-alkane chain.

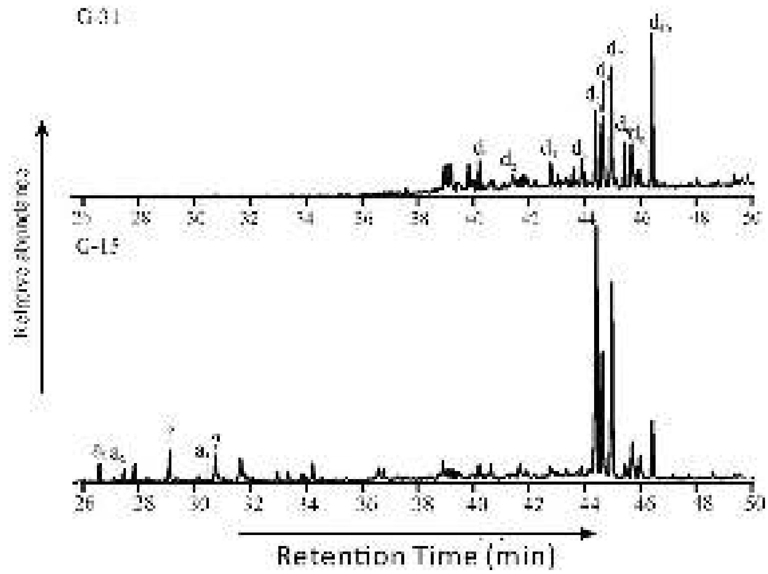

Fig. 12. Sesquiterpenoid and diterpenoid distribution *m/z* 123 the studied Gurha samples. Numbers correspond to compounds referred in Table 5.

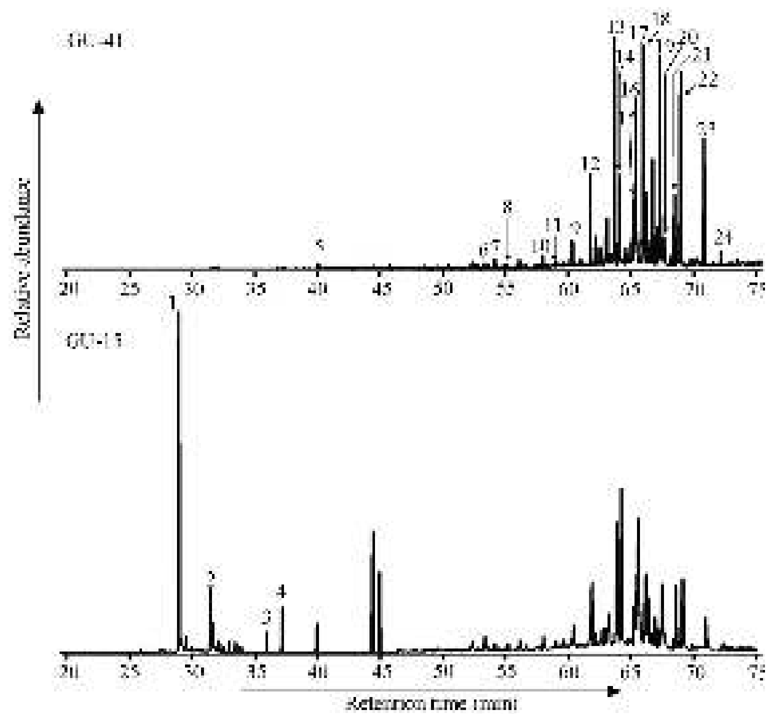

Fig. 13. Tricyclic and pentacyclic terpenoid distribution in the studied Gurha samples.

The S2 value shows the potential of a sample to generate hydrocarbons (especially oil) if it attained a sufficient maturity level to produce gaseous hydrocarbons (Tissot and Welte, 1984; Mendhe et al., 2017a, b). Rocks with S2 values > 4.0 mg HC/g rock are suggestive of a good source-rock. Thus, the obtained S2 values (16.30–247.88 mg HC/g, av. 112.55 mg HC/g) indicate that the Gurha samples have a very good ability to generate hydrocarbon. The hydrogen Index (HI) is also another critical parameter for the source rock quality (threshold value: 0.5 wt.%; Peters and Cassa, 1994; Hakimi et al., 2013; Hazra et al., 2015; Mendhe et al., 2017b, 2018b, c). The HI values for the samples vary between 101 and 546 mg HC/g TOC, and the OI values range from 31 to 91 mg CO_2/g TOC.

The studied samples have a low to moderate HI, and low OI values. The cross plots of HI and OI values demonstrate the information about the organic matter or kerogen type, the scattering of samples on the plot suggests that the sediments have mixed type III and II kerogens (Fig. 18a). Another cross plots like S2 vs. TOC (Fig. 18b) and HI vs. T_{max} (Fig. 18c) also show that the samples have an abundance of admixed type III-II kerogens (organic matter). Collectively, all these parameters advocate that the analyzed samples from Gurha mine have the ability to produce the gaseous to oil hydrocarbons.

Despite having sufficient TOC and suitable kerogen type, a source

Table 7
Biomarker parameters calculated for Gurha samples.

S. No.	CPI	TAR	Pr/Ph	Ph/*n*-C_{18}	Pr/*n*-C_{17}	P_{wax}	P_{aq}
G-41	2.55	5.93	0.7	0.39	0.13	0.39	0.83
G-32	2.23	2.35	0.97	0.96	0.43	0.52	0.74
G-31	5.5	56.2	3.13	0.26	3.19	0.22	0.94
G-15	2.65	2.66	1.36	0.3	0.17	0.58	0.74
G-9	5.97	37.58	2.31	0.33	1.08	0.27	0.9
G-2	7.01	22.22	1.17	0.65	0.95	0.22	0.92
Min.	**2.23**	**2.35**	**0.7**	**0.26**	**0.13**	**0.22**	**0.74**
Max.	**7.01**	**56.2**	**3.13**	**0.96**	**3.19**	**0.58**	**0.94**
Avg.	**4.32**	**21.16**	**1.61**	**0.48**	**0.99**	**0.37**	**0.85**

CPI (Carbon Preference Ratio) = $2(C_{23}+C_{25}+C_{27}+C_{29})/(C_{22}+2(C_{24}+C_{26}+C_{28})+C_{30})$ (Peters and Moldwan, 1993).
TAR (Terrigenous/Aquatic Ratio) = $(C_{27}+C_{29}+C_{31})/(C_{15}+C_{17}+C_{19})$ (Bourbonniere and Meyers, 1996).
P_{wax} (Proxy wax) = $(C_{27}+C_{29}+C_{31})/(C_{23}+C_{25}+C_{27}+C_{29}+C_{31})$ (Zheng et al., 2007).
P_{aq} (Proxy aqueous) = $(C_{23}+C_{25})/(C_{23}+C_{25}+C_{29}+C_{31})$ (Ficken et al., 2000).
Pr: Pristane; Ph: Phytane.

Table 8
Results of Rock-Eval pyrolysis of the Gurha samples.

Lithology	S. No.	S1	S2	S3	TOC	T_{max}	HI	OI	PI	GP	S2/S3
Shale	G-43	1.32	80.31	5.15	15.7	429	512	33	0.02	81.63	15.59
	G-41	1	46.37	5.97	13.03	428	356	46	0.02	47.37	7.77
	G-38	0.64	16.3	14.74	16.11	415	101	91	0.04	16.94	1.11
	G-35	2.96	143.45	15.27	35.56	421	403	43	0.02	146.41	9.39
	G-32	1.82	214.39	12.29	39.26	418	546	31	0.01	216.21	17.44
	Min.	**0.64**	**16.3**	**5.15**	**13.03**	**415**	**101**	**31**	**0.01**	**16.94**	**1.11**
	Max.	**2.96**	**214.39**	**15.27**	**39.26**	**429**	**546**	**91**	**0.04**	**216.21**	**17.44**
	Avg.	**1.55**	**100.16**	**10.68**	**23.93**	**422**	**384**	**49**	**0.02**	**101.71**	**10.26**
Lignite	G-31	1.09	63.59	21.39	39.15	418	193	34	0.02	64.68	2.97
	G-28	2.19	72.39	26.07	58.06	408	125	45	0.03	74.58	2.78
	G-23	1.2	247.88	20.61	52.09	427	476	40	0	249.08	12.03
	G-21	1.57	76.36	13.47	39.51	414	193	34	0.02	77.93	5.67
	G-17	9.5	104.63	22.24	58.76	405	178	38	0.08	114.13	4.7
	G-12	10.12	107.63	22.84	58.09	397	185	39	0.09	117.75	4.71
	G-9	1.47	160.95	16.52	44.32	418	363	37	0.01	162.42	9.74
	G-2	16.05	128.86	20.99	52.95	395	243	40	0.11	144.91	6.14
	Min.	**1.09**	**63.59**	**13.47**	**39.15**	**395**	**125**	**34**	**0**	**64.68**	**2.78**
	Max.	**16.05**	**247.88**	**26.07**	**58.76**	**427**	**476**	**45**	**0.11**	**249.08**	**12.03**
	Avg.	**5.4**	**120.29**	**20.52**	**50.37**	**410**	**245**	**38**	**0.05**	**125.69**	**6.09**

S1 = free hydrocarbons (mg HC/g); S2 = amount of hydrocarbons (mg HC/g); S3 = released carbon dioxide (mg CO_2/g); TOC = Total organic carbon (wt.%); T_{max} = temperature maximum (°C); OI (Oxygen Index) = (S3/TOC) × 100 (mg CO_2/g TOC); HI (Hydrogen Index) = (S2/TOC) × 100 (mg HC/g TOC); PI (Production Index) = S1/(S1+S2); GP (Genetic Potential) = S1+S2; S2/S3 =Hydrogen richness.

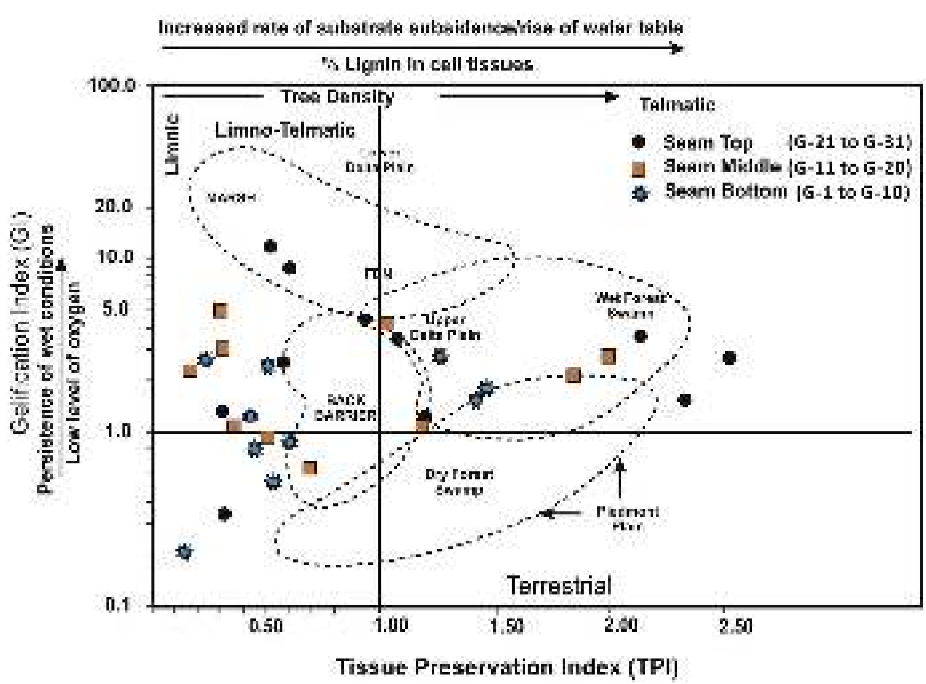

Fig. 14. Coal-facies diagram of the gelification index (GI) and tissue preservation index (TPI) in relation to depositional setting and type of mire (after Diessel, 1992).

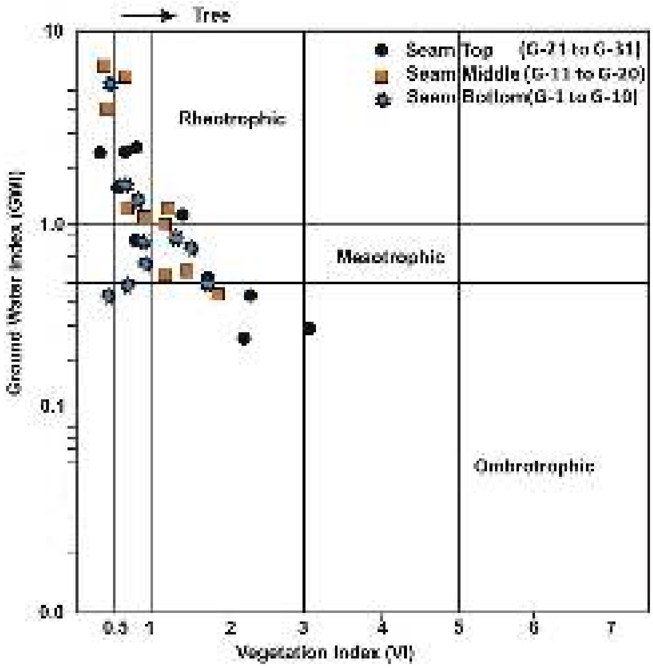

Fig. 15. Coal-facies diagram of vegetation index (VI) versus ground water index (GWI) plot showing palaeoenvironmental conditions (after Calder et al., 1991).

rock cannot generate hydrocarbon unless it is buried to sufficient depth for the organic material to attain thermal maturity. The evaluation of thermal maturity attained can be done based on the pyrolysis T_{max}, PI (potential index) and R_r (huminite reflectance). The T_{max} values can be used to determine the maturation of samples with TOC>0.5 wt.% and sufficient S2 yield (c.f. Akhande et al., 2012). The studied samples showed average T_{max} of 414 °C indicating immaturity. However, the T_{max} is highly sensitive to the kinetic behavior of macerals; it can vary depending on the compositions (Snowdown, 1995). Hence, in comparison with other parameters such as PI or R_r can give a more reliable result. The PI is considered as significant if the value is higher than 0.05%–0.1% (Garcia-Vallés et al., 2000). All the Gurha samples showed PI values < 0.05, which correspond to the immaturity of the samples. The measured T_{max} values and PI are also in good agreement with the R_r values.

Furthermore, in general, the values of huminite/vitrinite reflectance are being used for the assessment of wet and dry hydrocarbon generation potential of the organic matter. The reflectance values below 0.45 are suitable for the "heavy hydrocarbons" generation (Makhopadhyay, 1994). The random reflectance (R_r) values are varying between 0.20% and 0.47%, with maximum mean value 0.35% (Table 2), signifying that the studied lignites are prone for "heavy hydrocarbons" genesis.

Additionally, the occurrence of hop-17(21)-ene (thermally unstable compound) and relatively high incidence of ββ-hopane and points towards the limited hopanoid alteration, and the thermal immaturity of the organic matters (Petersen et al., 2004). The occurrences of the non-hopanoid triterpenoids compound with lupane or ursane, and the oleanane framework further indicates the immature nature of the studied organic matter (ten Haven et al., 1992). Moreover, the particulate OM data can also be useful in retrieving the information about hydrocarbon generation potential. The phytoclasts elements generally have the low hydrogen content (Batten, 1996b) and their relative abundance in the studied samples, thus indicate rather the low hydrocarbon generation ability (Tyson, 1995). In contrast, the AOM contents are rich in hydrogen (than carbon) component of OM and formed primarily in an anoxic condition (appropriate for source rock deposition; Pacton et al., 2011).

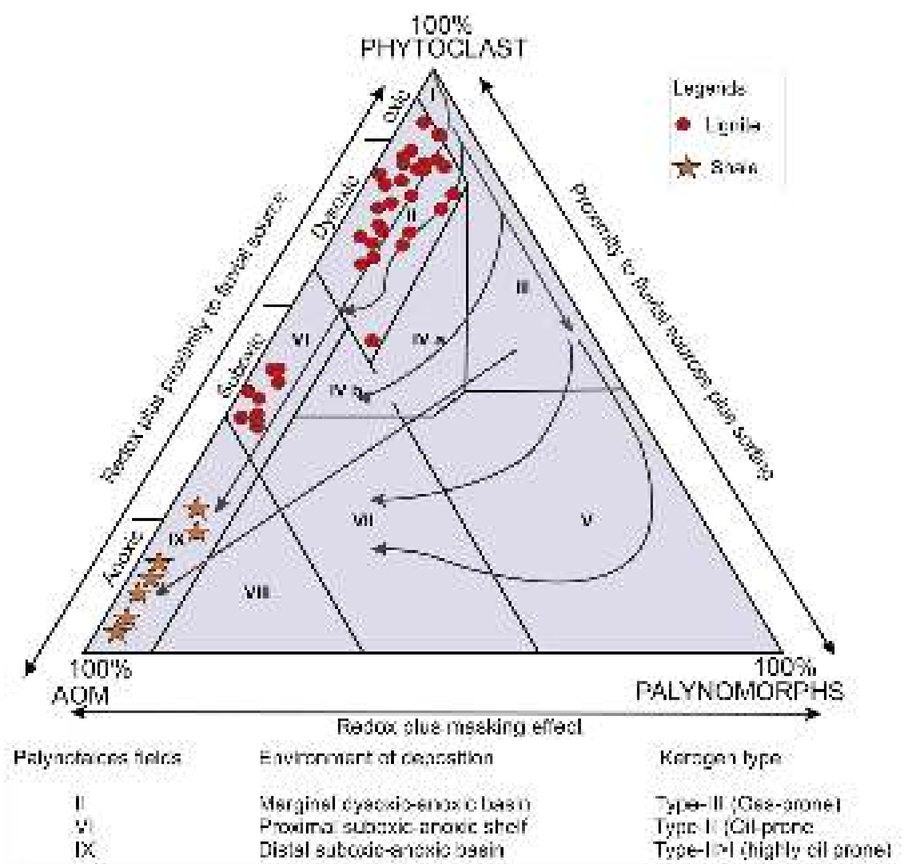

Fig. 16. Amorphous organic matter-palynomorph-phytoclast (APP) diagram showing depositional fields, the environment of deposition and Kerogen type for the studied lignite and shale samples.

Table 9
Palynotaxa from Gurha lignite-bearing sequence and their ecology.

Affinities	Palynotaxa	Climate	Ecological group
Onagraceae	*Grevilloideaepites pachyeximus*	Warm temperate	Cosmopolitan, mixed deciduous
Arecaceae	*Palmaepollenites eocenicus*	Tropical subtropical	Coastal, Moist forest
Rhizophoraceae	*Paleosantalaceaepites primitava*	Tropical	True mangrove
Rhizophoraceae	Cf. *Paleosantalaceaepites primitava*	Tropical	True mangrove
Euphorbiaceae	*Tricolporocolumellites pilatus*	Tropical	Low land
Bombaceae	*Tricolporocolumellites pilatus*	Tropical subtropical	Warmer
Unknown	*Florschuetzia rajpardensis*	Tropical subtropical	Low land
Rubiaceae	*Fevitrieticolpites* sp.	Tropical temperate	Cosmopolitan
Ctenolophonaceae	*Retistephanocolpites multirimatus*	Tropical	Fresh water swamp
Ctenolophonaceae	*Ctenolophonidites* sp.	Tropical-subtropical	Fresh water, cosmopolitan
Meliaceae	*Meliapollis pachydermis*	Tropical	Low land
Schizaeceae	*Cicatricososporites* sp.	Tropical-subtropical	Cosmopolitan
Microthyraceae	*Multicellaesporites* sp.	Tropical	Cosmopolitan

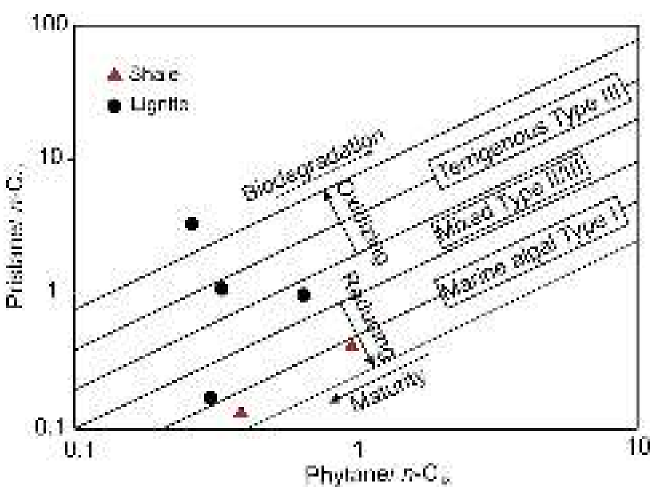

Fig. 17. Pristane/n-C_{17} vs. phytane/n-C_{18} plot of the samples from Gurha lignite mine.

Amorphous organic matter contents are vital for the generation for Type-II kerogens (Zhang et al., 2015), its appreciable amount in the samples, suggest a high-quality source-rock. Hence, the POM data exhibits that the Gurha lignite-bearing sequence can generate Type-III (mainly) and Type-II kerogens, also supported by the occurrence of reasonable content of perhydrous huminite + liptinite (10–70 vol.%; hydrogen-rich), in the lignites. It is also notable that the adjacent Palaeogene–Neogene basins/blocks like Barmer-Sanchore, Mehsana, Tharad, etc. are well known for oil and gas fields in India. Hence, the encouraging hydrocarbon potential of the studied lignites also inspires to explore the gas and oil exploration in the nearby equivalent geological formation.

6. Conclusions

A high-resolution study on the lignites and associated shales from Gurha lignite mine of northwestern Indian state Rajasthan have been carried out. The different data sets are corrobarated-well with each other

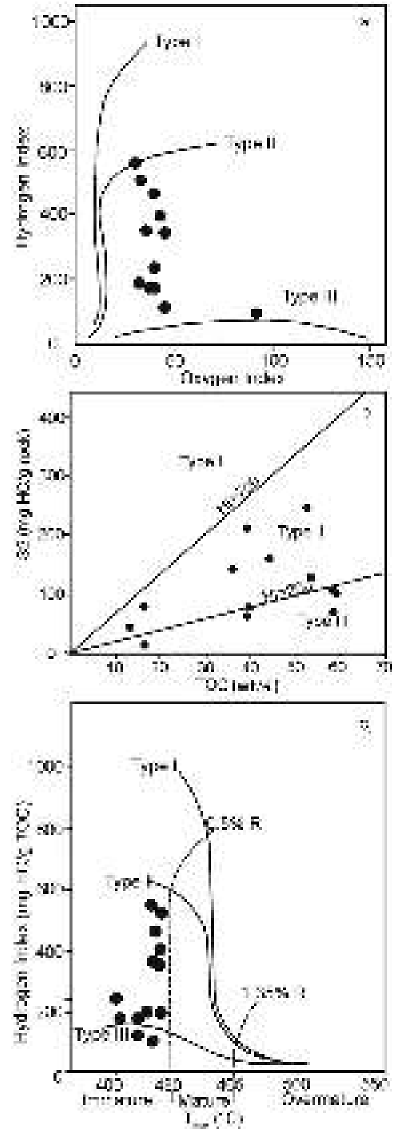

Fig. 18. Rock-Eval pyrolysis data of the samples of Gurha lignites; (a) HI vs. OI, (b) S2 vs. TOC, and (c) HI vs. T_{max} plots.

and to the prior research works. The following inferences have been deduced on the basis of detailed investigation:

I. The low-rank B lignites show that the palaeovegetation mainly comprised of higher plant (with some contribution of herbaceous vegetation) indicated by the dominance of huminite group, and phytoclasts and was subjected to bacterial degradation in time. The values of CPI and TAR further specify the significant terrigenous input.
II. The varieties of palaeo-flora (evergreen forests, freshwater swamps, mangroves) were thriving in a tropical-subtropical warm and humid climatic condition. However, the occurrence of gymnosperms points towards a temperate climatic zone in the vicinity.
III. The various petrographic indices suggest that the different ecological peat-forming plant groups were accumulated under limno-telmatic settings and in fluctuating (ombrotrphic to rheotrophic) hydrological conditions.
IV. The extrapolation of palynofacies data, Pr/n-C_{17} vs. Ph/n-C_{18} and Pr/Ph ratio together suggest that the sedimentation occurred mainly under oxic-dysoxic depositional environment with alternating fluctuations (suboxic) in a proximal setting. However,

distal suboxic-anoxic basin condition prevailed towards the termination of sedimentation.

V. Huminite reflectance (R_r), ββ-hopane, hop-17(21)-ene, non-hopanoid triterpenoids, T_{max} and PI indicate the thermal immaturity of organic matters.

VI. The dominance of terrestrial organic matters (huminite and phytoclasts) along with hydrogen rich AOM as well as the macerals data show the ability of these deposits to generate hydrocarbon (Kerogen type III//II).

VII. Sufficient TOC content and HI value indicate that these deposits have the potential to generate gaseous to oil hydrocarbon upon maturation. The low reflectance values favored for the generation of "heavy hydrocarbon".

Declaration of competing interest

The authors declare that they have no known competing financial interests or personal relationships that could have appeared to influence the work reported in this paper.

Acknowledgements

Authors are grateful to the Director, BSIP, Lucknow for his support, and granting consent to publish the data (BSIP/RDCC/20/2018-19). VPS is thankful to DST-SERB for providing the post-doctoral fellowship (PDF/2018/000883). We are also thankful to the VS Lignite Power Pvt. Ltd. officials for their help and support during the field visit. We also acknowledged the support extented by Mr. V.P. Singh, TO, BSIP, during laboratory investigation. Dr. Kristoffer Szilas, Associate Editor is thankfully acknowledged for his effective editorial support. We are also grateful to Prof. Dr. Dragana Životić and an anonymous reviewer for their constructive comments and valuable suggestions that bring more refinement to our work.

References

Akhande, S.O., Egenhoff, S.O., Obaje, N.G., Ojo, O.J., Adekeye, O.A., Erdtmann, B.D., 2012. Hydrocarbon potential of Cretaceous sediments in the lower and middle Benue trough, Nigeria: insights from new source rock facies. J. Afr. Earth Sci. 64, 34–47.
Alexander, R., Kagi, R.I., Noble, R., Volkman, J.K., 1984. Identification of some bicyclic alkanes in petroleum. Org. Geochem. 6, 63–70.
Ambwani, A.K., Singh, R.S., 1996. *Clavadiporopollenites raneriensis* gen. etsp. nov. from the Tertiary sediments of Bikaner District, Rajasthan, India. Palaeobotanist 43, 139–142.
Amijaya, H., Littke, R., 2005. Microfacies and depositional environment of Tertiary Tanjung Enim low rank coal, south Sumatra basin, Indonesia. Int. J. Coal Geol. 61, 197–221.
Ampaiwan, T., Churasiri, P., Kunwasi, C., 2003. Palynology of coal-bearing units in the Mae Ramat basin, Tak province, northern Thailand: implications for the paleoclimate and the paleoenvironment. Trop. Nat. Hist. 3, 19–40.
Aquino Neto, F.R., Trendel, J.M., Restle, A., Connan, J., Albrecht, P., 1983. Occurrence and formation of tricyclic and tetracyclic terpanes in sediments and petroleums. In: Bjorùy, M., et al. (Eds.), Advances in Organic Geochemistry. John Wiley and Sons, New York, pp. 659–676.
Azevedo, D.A., Aquino Neto, F.R., Simoneit, B.R.T., Pinto, A.C., 1992. Novel series of tricyclic aromatic terpanes characterized in Tasmanian tasmanite. Org. Geochem. 18, 9–16.
Batten, D.J., 1996. Palynofacies and palaeoenvironmental interpretation. In: Jansonius, J., Mc Gregor, D.C. (Eds.), Palynology: Principles and Applications, vol. 3. AASP, pp. 1011–1064.
Batten, D.J., Stead, D.T., 2005. Palynofacies analysis and its stratigraphic application. In: Koutsoukos, E.A.M. (Ed.), Applied Stratigraphy. Springer, Dordrecht, Netherlands, pp. 203–226.
Bechtel, A., Gruber, W., Sachsenhofer, R.F., Gratzer, R., Püttmann, W., 2001. Organic geochemical and stable isotopic investigation of coals formed in low-lying and raised mires within the Eastern Alps (Austria). Org. Geochem. 32, 1289–1310.
Bechtel, A., Sachsenhofer, R.F., Zdravkov, A., Kostova, I., Gratzer, R., 2005. Influence of floral assemblage, facies and diagenesis on petrography and organic geochemistry of the Eocene Bourgas coal and the Miocene Maritza-East lignite (Bulgaria). Org. Geochem. 36, 1498–1522.
Bhowmick, P.K., 2008. Phanerozoic petroliferous basin of India. Glimpses Geosci. Res. India 253–268.
Bordenave, M.L., 1993. Applied Petroleum Geochemistry. Editions Technip, Paris, p. 524.
Bourbonniere, R.A., Meyers, P.A., 1996. Sedimentary geo lipid records of historical changes in the watersheds and productivities of Lake Ontario and Erie. Limnol. Oceanogr. 41, 352–359.
Bujak, J.P., Barss, M.S., Williams, G.L., 1977. Offshore eastern Canada—Part I, Organic type and colour and hydrocarbon potential. Oil Gas J. 75, 198–201.
Calder, J.H., Gibbing, M.R., Mukhopadhyay, P.K., 1991. Peat formation in a Westphalian B piedmont setting, Cumberland Basin, Nova Scotia: implication for themaceral based interpretation of rheotrophic and raised paleomires. Bull. Soc. Geol. Fr. 162, 283–298.
Cameron, A.R., Kalkreuth, W., Koukouzas, C., 1984. The petrology of Greek brown coals. Int. J. Coal Geol. 4, 173–207.
Carvalho, M.A., Ramos, R.R.C., Crud, M.B., Witovisk, L., Kellner, A.W.A., Silva, H.P., Grillo, O.N., Riff, D., Romano, P.S.R., 2013. Palynofacies as indicators of paleoenvironmental changes in a Cretaceous succession from the Larsen basin, James Ross island, Antarctica. Sediment. Geol. 295, 53–66.
Clayton, J.L., 1993. Composition of crude oils generated from coals and organic matter in shale. In: Low, B.E., Rice, D.D. (Eds.), Hydrocarbons from Coal, AAPG Studies in Geology, vol. 38, pp. 85–198.
Corbet, B., Albrecht, P., Ourisson, G., 1980. Photochemical or photomimetic fossil triterpenoids in sediments and petroleum. J. Am. Chem. Soc. 102, 1171–1173.
Cranwell, P.A., 1977. Organic geochemistry of Cam Loch (Sutherland) sediments. Chem. Geol. 20, 205–221.
Cranwell, P.A., Eglinton, G., Robison, N., 1987. Lipids of aquatic organisms as potential contributors to lacustrine sediments—II. Org. Geochem. 11, 513–527.
Crosdale, P.J., 1993. Coal maceral ratios as indicators of environment of deposition: do they work for ombrogenous mires? An example from the Miocene of New Zealand. Org. Geochem. 20, 797–809.
Dai, S., Ren, D., Li, S., Zhao, L., Zhang, Y., 2007. Coal facies evolution of the main minable coal-bed in the Heidaigou Mine, Jungar Coalfield, Inner Mongolia, northern China. Science in China D. Earth Sci. Rev. 50, 144–152.
Dehmer, J., 1995. Petrological and organic geochemical investigation of recent peats with known environments of deposition. Int. J. Coal Geol. 28, 111–138.
Dev, S., 1989. Terpenoids. In: Rowe, J.W. (Ed.), Natural Products of Wood Plants 1. Springer, Berlin, pp. 691–807.
Didyk, B.M., Simoneit, B.R.T., Brassell, S.C., Eglinton, G., 1978. Organic geochemical indicators of paleoenvironmental conditions of sedimentation. Nature 272, 216–222.
Diessel, C.F.K., 1986. On the correlation between coal facies and depositional environments. In: Proc. 20th Newcastle Symp. The University of Newcastle, pp. 19–22.
Diessel, C.F.K., 1992. Coal-bearing Depositional Systems. Springer-Verlag, Berlin, p. 721.
Dow, W.G., Pearson, D.B., 1975. Organic matter in Gulf coast sediments. In: Reprints, Seventh Annual Offshore Technology Conference. Offshore Technology Conference, pp. 85–90.
Drobniak, A., Mastalerz, M., 2006. Chemical evolution of Miocene wood: example from the Belchatow brown coal deposit, central Poland. Int. J. Coal Geol. 66, 157–178.
Dutta, S., Mathews, R.P., Singh, B.D., Tripathi, S.K.M., Singh, A., Saraswati, P.K., Banerjee, S., Mann, U., 2011. Petrology, palynology and organic geochemistry of Eocene lignite of Matanomadh, Kutch Basin, western India: implications to depositional environment and hydrocarbon source potential. Int. J. Coal Geol. 85, 91–102.
Dutta, S.K., Sah, S.C.D., 1970. Palynostratigraphy of the Tertiary sedimentary formations of Assam-5. Stratigraphy and palynology of South Shilong Plateau. Palaeontographica Abt. B 131 (1-4), 1–72.
Espitalié, J., Laporte, J.L., Madec, M., Marquis, F., Leplat, P., Paulet, P., 1977. Méthode rapide de la caractérisation des roches méres de leur potentiel pétrolier et de leur degré dévolution. Rev. Fr. Pet. Inst. 32, 23–42 (in French with English abstract).
Ficken, K.J., Li, B., Swain, D.L., Eglinton, G., 2000. An *n*-alkane proxy for the sedimentary input of submerged/floating freshwater aquatic macrophytes. Org. Geochem. 31, 745–749.
Ficken, K.J., Wooller, M.J., Swain, D.L., Street-Perrott, F.A., Eglinton, G., 2002. Reconstruction of a subalpine grass-dominated ecosystem, Lake Rutundu, Mount Kenya: a novel multi-proxy approach. Paleogeogr. Paleoclimatol. Paleoecol. 177, 137–149.
Garcia-Vallés, M., Vendrell-Saz, M., Pradell-Cara, T., 2000. Organic geochemistry (Rock-Eval) and maturation rank of the Garumnian coal in the central Pyrenees (Spain). Fuel 79, 505–513.
Giger, W., Schaffner, C., Wakeham, S.G., 1980. Aliphatic and olefinic hydrocarbons in recent sediments of Greifensee, Switzerland. Geochem. Cosmochim. Acta 44, 119–129.
GSI (Geological Survey of India), 2011. Geology and Mineral Resources of Rajasthan, third ed., vol. 12. Miscellaneous Publication No. 30. 120(p).
Hakimi, M.H., Abdullah, W.H., Sia, S.G., Makeen, Y.M., 2013. Organic geochemical and petrographic characteristics of Tertiary coals in the northwest Sarawak, Malaysia: implications for palaeoenvironmental conditions and hydrocarbon generation potential. Mar. Pet. Geol. 48, 31–46.
Hatcher, P.G., Clifford, D.J., 1997. The organic geochemistry of coal: from plant material to coal. Org. Geochem. 27, 251–274.
Hazra, B., Varma, A.K., Bandopadhyay, A.K., Mendhe, V.A., Singh, B.D., Saxena, V.K., Samad, S.K., Mishra, D.K., 2015. Petrographic insights of organic matter conversion of Raniganj basin shales. India. International Journal of Coal Geology 150–151, 193–209.
Hoorn, C., Straathof, J., Abels, H.A., Xu, Y., Utescher, T., 2012. A late Eocene palynological record of climate change and Tibetan Plateau uplift (Xining Basin, China). Palaeogeogr. Palaeoclimatol. Palaeoecol. 344–345, 16–38.
Horsfield, B., Yordy, K.L., Crelling, J.C., 1988. Determining the petroleum generating potential of coal using geochemistry and organic petrology. Org. Geochem. 13, 121–129.
Hunt, J.M., 1996. Petroleum Geochemistry and Geology, second ed. Freeman, New York, p. 743.

ICCP, 2001. The new inertinite classification (ICCP system 1994), international committee for coal and organic petrology. Fuel 80, 459–471.
Iordanidis, A., Georgakopoulos, A., 2003. Pliocene lignites from Apofysis mine, Amynteo basin, Northwestern Greece: petrographical characteristics and depositional environment. Int. J. Coal Geol. 54, 57–68.
ISO, 2009. Methods for the Petrographic Analysis of Bituminous Coal and Anthracite—Part 2 (7404-2): Methods of Preparing Coal Samples, 8(p); Part 3 (7404-3): Methods of Determining Maceral Group Composition, 4(p); Part 5 (7404-5): Methods of Determining Microscopically the Reflectance of Vitrinite, 11(p). International Organization for Standardization, ISO, Geneva.
ISO-11760, 2005. Classification of coals. Int. Stand. 1–9.
Jacob, J., Disnar, J.-R., Boussafir, M., Albuquerque, A.L.S., Sifeddine, A., Turcq, B., 2007. Contrasted distributions of triterpene derivatives in the sediments of Lake Caçó reflect paleoenvironmental changes during the last 20,000 yrs in NE Brazil. Org. Geochem. 38, 180–197.
Jain, K.P., Kar, R.K., Sah, S.C.D., 1973. A palynological assemblage from Barmer, Rajasthan. Geophytol 3 (2), 150–165.
Jasper, K., Krooss, B.M., Flajs, G., Hartkopf-Fröder, C., Littke, R., 2009. Characteristics of type III kerogen in coal-bearing strata from the Pennsylvanian (Upper Carboniferous) in the Ruhr Basin, Western Germany: comparison of coals dispersed organic matter, kerogen concentrates and coal-mineral mixtures. Int. J. Coal Geol. 80, 1–19.
Kalaitzidis, S., Bouzinos, A., Christanis, K., 2000. Paleoenvironment of Lignite Formation Prior to and after the Deposition of the "Characterstic Sand" in the Lignite Deposit of Ptolemais, vol. 115. Mineral Wealth, Athens, pp. 29–42.
Kalgutkar, R.M., Jansonius, J., 2000. Synopsis of fungal spores, mycelia and fructifications. AASP Contribution Series 39, 1–423.
Kalkreuth, W., Kotis, T., Papanikolaou, C., Kokkinakis, P., 1991. The geology and coal petrology of a Miocene lignite profile at Meliadi Mine, Katerini, Greece. Int. J. Coal Geol. 17, 51–67.
Kar, R.K., 1995. *Diporocolpis*: a new type of aperture from the early Eocene sediments of Rajasthan, India. Palaeobotanist 42, 380–386.
Kar, R.K., 1996. Late Cretaceous and Tertiary palynological succession in India. Palaeobotanist (Lucknow) 45, 71–80.
Kar, R.K., Saxena, R.K., 1976. Algal and fungal microfossils from Matanomadh Formation (Palaeocene), Kutch, India. The Palaeobot 23 (1), 1–15.
Kar, R.K., Sharma, P., 2001. Palynostratigraphy of late Palaeocene and early Eocene sediments of Rajasthan, India. Palaeontogr. Abt B 256, 123–157.
Kar, R.K., Singh, R.Y., Sah, S.C.D., 1972. On some algal and fungal remains from Tura Formation of Garo Hills, Assam. The Palaeobot 19, 146–154.
Karrer, W., Cherbuliez, E., Eugster, C.H., 1977. Konstitution und vorkommen der organischen Pflanzenstoffe (exclusive Alkaloide) Ergänzungsband, vol. 1. Birkhäuser Verlag, Basel (in German).
Kotarba, M., Clayton, J., Rice, D., Wagner, M., 2002. Assessment of hydrocarbon source rock potential of Polish bituminous coals and Carbonaceous shales. Chem. Geol. 184, 11–35.
Kumar, M., Spicer, R.A., Spicer, T.E.V., Shukla, A., Mehrotra, R.C., Monga, P., 2016. Palynostratigraphy and palynofacies of the early Eocene Gurha lignite mine, Rajasthan, India. Palaeogeogr. Palaeoclimatol. Palaeoecol. 461, 98–108.
Kumar, J., Mendhe, V.A., Bannerjee, M., Mishra, S., Mishra, V.K., Singh, P.K., Singh, H., 2018. Coalbed methane reservoir characteristics of coal seams of South Karanpura Coalfield, Jharkhand, India. Int. J. Coal Geol. 196, 185–200.
Lafargue, E., Marquis, F., Pillot, D., 1998. Rock-Eval–6 applications in hydrocarbon exploration, production and soil contamination studies. Oil Gas Sci. Technol. 53, 421–437.
Littke, R., Horsfield, B., Leythaeuser, D., 1989. Hydrocarbon distribution in coals and dispersed organic matter of different maceral compositions and maturities. Geol. Rundsch. 78, 391–410.
Makhopadhyay, P.K., 1994. Vitrinite reflectance as maturity parameter petrographic and molecular characterization and its applications to basin modeling (chapter 1). In: Makhopadhyay, P.K., Dow, W.G.((Eds.), Vitrinite Reflectance as a Maturity Parameter Applications and Limitations. ACS Symposium Series. American Chemical Society, Washington DC, pp. 1–23.
Mandal, J., 1990. Palynological investigation of Palaeocene sediments from Thanjinath, Meghalaya. The Palaeobot 37 (3), 324–330.
Mehrotra, R.C., Shukla, A., 2019. First record of Dioscorea from the early Eocene of northwestern India: its evolutionary and palaeoecological importance. Rev. Palaeobot. Palynol. 261, 11–17.
Mendhe, V.A., Mishra, S., Varma, A.K., Kamble, A.D., Bannerjee, M., Sutay, T.M., 2017a. Gas reservoir characteristics of the lower Gondwana Shales in Raniganj basin of eastern India. J. Pet. Sci. Eng. 149, 649–664.
Mendhe, V.A., Bannerjee, M., Varma, A.K., Kamble, A.D., Mishra, S., Singh, B.D., 2017b. Fractal and pore dispositions of coal seams with significance to coalbed methane plays of east Bokaro, Jharkhand, India. J. Nat. Gas Sci. Eng. 38, 412–433.
Mendhe, V.A., Mishra, S., Varma, A.K., Bannerjee, M., Singh, B.D., Singh, V.P., 2018a. Geochemical and petrophysical characteristics of Permian shale gas reservoirs of Raniganj Basin, West Bengal, India. Int. J. Coal Geol. 188, 1–24.
Mendhe, V.A., Kumar, V., Saxena, V.K., Bannerjee, M., Kamble, A.D., Singh, B.D., Mishra, S., Sharma, S., Kumar, J., Varma, A.K., Mishra, D.K., Samad, S.K., 2018b. Evaluation of gas resource potentiality, geochemical and mineralogical characteristics of Permian shale beds of Latehar-Auranga Coalfield, India. Int. J. Coal Geol. 196, 43–62.
Mendhe, V.A., Kumar, S., Kamble, A.D., Mishra, S., Varma, A.K., Bannerjee, M., Mishra, V.K., Sharma, S., Buragohain, J., Tiwari, B., 2018c. Organo-mineralogical insights of shale gas reservoir of Ib-River Mand-Raigarh basin, India. J. Nat. Gas Sci. Eng. 59, 136–155.
Mendonça Filho, J.G., Mendonça, J.O., Menezes, T.R., Oliveira, A.D., Carvalho, M.A., Santanna, A.J., Souza, J.T., 2010. Palinofácies. In: Carvalho, I.S. (Ed.), Paleontologia, third ed., vol. 1. Interciência, Rio de Janeiro, pp. 379–413 (in Portuguese with English abstract).
Mendonça Filho, J.G., Menezes, T.R., Mendonça, J.O., 2011. Organic composition (palynofacies analysis). In: ICCP Training Course on Dispersed Organic Matter, pp. 33–81 (Chapter 5).
Mendonça Filho, J.G., Menezes, T.R., Mendonça, J.O., Oliveira, A.D., Silva, T.F., Rondon, N.F., Da Silva, F.S., 2012. Organic facies: palynofacies and organic geochemistry approaches. In: Panagiotaras, D. (Ed.), Geochemistry-Earth's System Processes. InTech, pp. 211–248.
Moldowan, J.M., Seifert, W.K., Gallegos, E.J., 1985. Relation between petroleum composition and depositional environment of petroleum source. AAPG Bull. 69, 1255–1268.
Moore, T.A., Shearer, J.C., 2003. Peat/coal type and depositional environment-are they related? Int. J. Coal Geol. 56, 233–252.
Naafs, B.D.A., Rohrssen, M., Inglis, G.N., Lähteenoja, O., Feakins, S.J., Collinson, M.E., Kennedy, E.M., Singh, P.K., Singh, M.P., Lunt, D.J., Pancost, R.D., 2018. High temperatures in the terrestrial mid-latitudes during the early Palaeogene. Nat. Geosci. 11, 766–771.
Navale, G.K.B., Misra, B.K., 1979. Some new pollen grains from Neyveli lignite, Tamil Nadu, India. Geophytol. 8 (2), 226–239.
Nip, M., De Leeuw, J.W., Schenck, P.A., Meuzelaar, H.L.C., Stout, S.A., Given, P.H., Boon, J.J., 1985. Curie–point pyrolysis mass spectrometry, Curie-point pyrolysis-gas chromatography-mass spectrometry and fluorescence microscopy as analytical tools for the characterization of two uncommon lignites. J. Anal. Appl. Pyrolysis 8, 221–239.
Noble, R.A., Alexander, R., Kag, R.I., Knox, J., 1985. Tetracyclic diterpenoid hydrocarbons in some Australian coals, sediments and crude oils. Geochem. Cosmochim. Acta 49, 2141–2147.
Oikonomopoulos, I.K., Perraki, M., Tougiannidis, N., Perraki, T., Frey, M.J., Antoniadis, P., Ricken, W., 2013. A comparative study on structural differences of xylite and matrix lignite lithotypes by means of FT-IR, XRD, SEM and TGA analyses: an example from the Neogene Greek lignite deposits. Int. J. Coal Geol. 115, 1–12.
Otto, A., Wilde, V., 2001. Sesqui-, di-, and triterpenoids as chemosystematic markers in extant conifers- a review. Bot. Rev. 67, 141–238.
Otto, A., Walther, H., Püttmann, W., 1997. Sesqui- and diterpenoid biomarkers preserved in Taxodium-rich Oligocene oxbow lake clays, Weisselster Basin, Germany. Org. Geochem. 26, 105–115.
Pacton, M., Gorin, G.E., Vasconcelos, C., 2011. Amorphous organic matter – experimental data on formation and the role of microbes. Rev. Palaeobot. Palynol. 166, 253–267.
Paul, S., Dutta, S., 2016. Terpenoid composition of fossil resins from western India: new insights into the occurrence of resin-producing trees in Early Paleogene equatorial rainforest of Asia. Int. J. Coal Geol. 167, 65–74.
Paul, S., Sharma, J., Singh, B.D., Saraswati, P.K., Dutta, S., 2015. Early Eocene equatorial vegetation and depositional environment: biomarker and palynological evidences from a lignite-bearing sequence of Cambay Basin, western India. Int. J. Coal Geol. 149, 77–92.
Pereira, R., Carvalho, I.S., Simoneit, B.R.T., Azevedo, D.A., 2009. Molecular composition and chemosystematic aspects of Cretaceous amber from the Amazonas, Araripe and Recôncavo basins, Brazil. Org. Geochem. 40, 863–875.
Peters, K.E., 1986. Guidelines for evaluating petroleum source rock using programmed pyrolysis. AAPG Bull. 70, 318–386.
Peters, K.E., Cassa, M.R., 1994. Applied source rock geochemistry. In: Magoon, L.B., Dow, W.G. (Eds.), The Petroleum System from Source to Trap, vol. 60. AAPG Memoir, pp. 93–120.
Peters, K.E., Moldowan, J.M., 1993. The Biomarker Guide. Interpreting Molecular Fossils in Petroleum and Ancient Sediments. Prentice Hall, NJ, USA, p. 363.
Peters, K.E., Walters, C.C., Moldowan, J.M., 2005. The Biomarker Guide. Cambridge University, New York, p. 1132.
Peters, A.D., Agama, C.I., Asiedu, D.K., Apesegah, E., 2013. Palynology, palynofacies and Palaeoenvironments of sedimentary organic matter from Bonyere - 1 well, Tano basin, western Ghana. Int. Lett. Nat. Sci. 5, 27–45.
Petersen, H.I., Nytoft, H.P., Nielsen, L.H., 2004. Characterisation of oil and potential source rocks in the north-eastern Song Hong Basin, Vietnam: indications of a lacustrine-coal sourced petroleum system. Org. Geochem. 35, 493–515.
Philp, R.P., 1985. Fossil fuel markers. In: Methods in Geochemistry and Geophysics, vol. 23. Elsevier, p. 294.
Pickel, W., Kus, J., Flores, D., Kalaitzidis, S., Christanis, K., Cardott, B.J., Misz-Kennan, M., Rodrigues, S., Hentschel, A., Hamor-Vido, M., Crosdale, P., Wagner, N., ICCP, 2017. Classification of liptinite – ICCP system 1994. Int. J. Coal Geol. 169, 40–61.
Powell, T.G., 1988. Pristane/phytane ratio as environmental indicator. Nature 333, 604.
Prasad, B., Asher, R., Borgohai, B., 2010. Late Neoproterozoic (Ediacaran)-Early Paleozoic (Cambrian) achritarchs from the Marwar supergroup, Bikaner-Nagaur Basin, Rajasthan. J. Geol. Soc. India 75, 415–431.
Rajak, P.K., Singh, V.K., Singh, P.K., Singh, M.P., Singh, A.K., 2019. Environment of paleomire of lignite seams of Bikaner Nagaur basin, Rajasthan (W. India): petrological implications. Int. J. Oil Gas Coal Technol. 22 (2), 218–245.
Raju, S.V., Mathur, N., Sarmah, M.K., 2014. Geochemical characterization of Neoproterozoic heavy oil from Rajasthan, India: implications for future exploration of hydrocarbons. Curr. Sci. 107, 1298–1305.
Sah, S.C.D., Kar, R.K., 1974. Palynology of the Tertiary sediments of Palana, Rajasthan. Palaeobotanist 21, 163–188.
Sah, S.C.D., Kar, R.K., Singh, R.Y., 1971. Stratigraphic range of Dandotiaspora gen. nov. in the Lower Eocene sediments of India. Geophytol 1, 54–63.

Saxena, R.K., 1978. Palynology of the Matanomadh Formation in type area, north-western Kutch, India (Part 1). Systematic description of pteridophytic spores. The Palaeobot 25, 448–456.
Saxena, R.K., 1979. Reworked Cretaceous spores and pollen grains from the Matanomadh Formation (Palaeocene), Kutch, India. The Palaeobot 26 (2), 167–174.
Saxena, R.K., 1982. Taxonomic study of the polycolpate pollen grains from the Indian Tertiary sediments with special reference to nomenclature. Rev. Palaeobot. Palynol 37 (3-4), 183–315.
Scott, A.C., 2002. Coal petrology and the origin of coal macerals: a way ahead? Int. J. Coal Geol. 50, 119–134.
Shukla, A., Mehrotra, R.C., 2014. Paleoequatorial rain forest of western India during the EECO: evidence from Uvaria L. fossil and its geological distribution pattern. Hist. Biol. 26 (6), 693–698.
Shukla, A., Mehrotra, R.C., 2016. Early Eocene (~50 My) legume fruits from Rajasthan. Curr. Sci. 11, 465–467.
Shukla, A., Mehrotra, R.C., 2018. Early Eocene plant megafossil assemblage of western India: paleoclimatic and paleobiogeographic implications. Rev. Palaeobot. Palynol. 258, 123–132.
Shukla, A., Mehrotra, R.C., Spicer, R.A., Spicer, T.E.V., Kumar, M., 2014. Cool equatorial terrestrial temperatures and the south Asian monsoon in the early Eocene: evidence from the Gurha mine, Rajasthan, India. Paleogeogr. Paleoclimatol. Paleoecol. 412, 187–198.
Shukla, A., Mehrotra, R.C., Ali, S.N., 2018. Early Eocene leaves of northwestern India and their response to climate change. J. Asian Earth Sci. 166, 152–161.
Silva, M.B., Kalkreuth, W., Holz, M., 2008. Coal petrology of coal seams from the Leão-Butiá coalfield, lower Permian of the Paraná basin, Brazil: implications for coal facies interpretations. Int. J. Coal Geol. 73, 331–358.
Singh, R.Y., Dogra, N.N., 1988. Palynological zonation of Palaeocene of India with special reference to western Rajasthan. In: Maheshwari, H.K. (Ed.), Proc. Symp. Palaeocene of India: Limits and Subdivisions, 1986. Indian Assoc. Palynostratigraphers, Lucknow, pp. 51–64.
Singh, A.K., Kumar, A., 2018. Petrographic and geochemical study of GurhaLignites, Bikaner basin, Rajasthan, India: implications for thermal maturity, hydrocarbon generation potential and paleodepositional environment. J. Geol. Soc. India 92, 27–35.
Singh, A., Misra, B.K., 1991. Revision of some Tertiary pollen genera and species. Rev. Palaeobot. Palynol 67 (3-4), 205–215.
Singh, A., Misra, B.K., Singh, B.D., Navale, G.K.B., 1992. The Neyveli lignite deposits (Cauvery Basin), India: organic composition, age and depositional pattern. Int. J. Coal Geol. 21, 45–97.
Singh, H., Prasad, M., Kumar, K., Singh, S.K., 2011. Palaeobotanical remains from the Palaeocene-Lower Eocene Vagadkhol Formation, western India, and their palaeoclimatic and phytogeographic implications. Palaeoworld 20, 332–356.
Singh, A., Mahesh, S., Singh, H., Tripathi, S.K.M., Singh, B.D., 2013. Characterization of Mangrol lignite (Gujarat), India: petrography, palynology, and palynofacies. Int. J. Coal Geol. 120, 82–94.
Singh, H., Prasad, M., Kumar, K., Singh, S.K., 2015a. Early Eocene macroflora and associated palynofossils from the Cambay Shale formation, western India: phytogeographic and palaeoclimatic implications. Palaeoworld 24, 293–323.
Singh, P.K., Rajak, P.K., Singh, M.P., Naik, A.S., Singh, V.K., Raju, S.V., Ojha, S., 2015b. Environmental geochemistry of selected elements in lignite from Barsingsar and Gurha mines of Rajasthan, western India. J. Geol. Soc. India 86, 23–32.
Singh, P.K., Rajak, P.K., Singh, V.K., Singh, M.P., Naik, A.S., Raju, S.V., 2016. Studies on thermal maturity and hydrocarbon potential of lignites of Bikaner–Nagaur basin, Rajasthan. Energy Explor. Exploit. 34 (1), 140–157.
Singh, A., Shivanna, M., Mathews, R.P., Singh, B.D., Singh, H., Singh, V.P., Dutta, S., 2017a. Paleoenvironment of Eocene lignite bearing succession from Bikaner-Nagaur Basin, western India: organic petrography, palynology, palynofacies and geochemistry. Int. J. Coal Geol. 181, 87–102.
Singh, V.P., Singh, B.D., Singh, A., Singh, M.P., Mathews, R.P., Dutta, S., Mendhe, V.A., Mahesh, S., Mishra, S., 2017b. Depositional palaeoenvironment and economic potential of Khadsaliya lignite deposits (Saurashtra Basin), western India: based on petrographic, palynofacies and geochemical characteristics. Int. J. Coal Geol. 171, 223–242.
Singh, V.P., Singh, B.D., Mathews, R.P., Singh, A., Mendhe, V.A., Singh, P.K., Mishra, S., Dutta, S., Shivanna, M., Singh, M.P., 2017c. Investigation on the lignite deposits of Surkha mine (Saurashtra Basin, Gujarat), western India: their depositional history and hydrocarbon generation potential. Int. J. Coal Geol. 183, 78–99.
Singh, V.K., Rajak, P.K., Singh, P.K., 2018. Revisiting the paleomires of western India: an insight into the early Paleogene lignite Corridor. J. Asian Earth Sci. https://doi.org/10.1016/j.jseaes.2018.08.031.
Sinha-Roy, S., Malhotra, G., Mohanti, M., 1998. Geology of Rajasthan. Geological Society of India, Bangalore, p. 278.
Smyth, M., Xu Jian, F., Ward, C.R., 1992. Potential petroleum source rocks in Triassic lacustrine-delta sediments of the Gunnedah Basin, Eastern Australia. J. Pet. Geol. 15, 435–450.
Snowdon, L.R., 1995. Rock-eval T_{max} suppression: documentation and amelioration. AAPG Bull. 79, 1337–1348.
Stefanova, M., Markova, K., Marinov, S., 2002. Molecular indicators for coal-forming palaeoplant community. "Katrishte'' coal deposit. Proc. IV Euro. Coal Conf. Polish Geological Institute Special Papers 7, 245–252.
Suárez-Ruiz, I., Flores, D., Mendonça Filho, J.G., Hackley, P.C., 2012. Review and update of the applications of organic petrology: Part 1, Geological applications. Int. J. Coal Geol. 22, 54–112.
Summerhayes, C.P., 1983. Sedimentation of organic matter in upwelling regimes. In: Thiede, J., Suess, E. (Eds.), Coastal Upwelling: its Sediments Record Part B: Sedimentary Records of Ancient Coastal Upwelling. Plenum Press, New York, pp. 29–72.
Sykes, R., Snowdon, L., 2002. Guidelines for assessing the petroleum potential of coaly source rocks using Rock-Eval pyrolysis. Org. Geochem. 33 (12), 1441–1455.
Sýkorová, I., Pickel, W., Christanis, K., Wolf, M., Taylor, G.H., Flores, D., 2005. Classification of huminite— ICCP system 1994. Int. J. Coal Geol. 62, 85–106.
Taylor, G.H., Teichmüller, M., Davis, A., Diessel, C.F.K., Littke, R., Robert, P., 1998. Organic Petrology. GebrüderBorntraeger, Berlin, p. 704.
Teichmüller, M., 1989. The genesis of coal from the view point of coal petrology. Int. J. Coal Geol. 12, 1–87.
ten Haven, H.L., Peakman, T.M., Rullkotter, J., 1992. δ2-Triterpenes: early intermediates in the diagenesis of terrigenous triterpenoids. Geochem. Cosmochim. Acta 56, 1993–2000.
Tissot, B.P., Welte, D.H., 1984. Petroleum Formation and Occurrence, second ed. Springer, Berlin-Heidelberg-New York, p. 669.
Traverse, A., 1988. Palaeopalynology. Unwin Hyman Ltd., London, p. 600.
Trendel, J.M., Lohmann, F., Kintzinger, J.P., Albrecht, P., 1989. Identification of des-A-triterpenoid hydrocarbons occurring in surface sediments. Tetrahedron 45, 4457–4470.
Tyson, R.V., 1995. Sedimentary Organic Matter: Organic Facies and Palynofacies. Chapman & Hall, London, p. 615.
Varma, A.K., Hazra, B., Chinara, I., Mendhe, V.A., Dayal, A.M., 2015. Assessment of organic richness and hydrocarbon generation potential of Raniganj basin shales, West Bengal, India. Mar. Pet. Geol. 59, 480–490.
Varma, A.K., Mishra, D.K., Samad, S.K., Prasad, A.K., Panigrahi, D.C., Mendhe, V.A., Singh, B.D., 2018. Geochemical and organo-petrographic characterization for hydrocarbon generation from Barakar formation in Auranga basin, India. Int. J. Coal Geol. 186, 97–114.
Venkatachala, B.S., Kar, R.K., 1969. Palynology of the Tertiary sediments of Kutch-1. Spores and pollen from the bore hole no. 14. The Palaeobot 17 (2), 157–178.
Waples, D.W., Machihara, T., 1991. Biomarkers for geologists: a practical guide to the application of steranes and triterpanes in petroleum geology. AAPG Methods Explor. 9, 19–40.
Weston, R.J., Philp, R.P., Sheppard, C.M., Woolhouse, A.D., 1989. Sesquiterpanes, diterpanes and other higher terpanes in oils from the Taranaki Basin of New Zealand. Org. Geochem. 14, 405–421.
Wilkins, W.T., George, S.C., 2002. Coal as a source rock for oil: a review. Int. J. Coal Geol. 50, 317–361.
Wüst, R.A.J., Hawke, M.I., Bustin, R.M., 2001. Comparing maceral ratios from tropical peat lands with assumptions from coal studies: do classic coal petrographic interpretation methods have to be discarded? Int. J. Coal Geol. 48, 115–132.
Zdravkov, A., Bechtel, A., Sachsenhofer, R.F., Kortenski, J., Gratzer, R., 2011. Vegetation differences and diagenetic changes between two Bulgarian lignite deposits: insights from coal petrology and biomarker composition. Org. Geochem. 42, 237–254.
Zhang, M., Ji, L., Wu, Y., He, C., 2015. Palynofacies and geochemical analysis of the Triassic Yanchang Formation, Ordos Basin: implications for hydrocarbon generation potential and the paleoenvironment of continental source rocks. Int. J. Coal Geol. 152, 159–176.
Zheng, Y., Zhou, W., Meyers, P.A., Xie, S., 2007. Lipid biomarkers in the Zoigê–Hongyuan peat deposit: indicators of Holocene climate changes in West China. Org. Geochem. 38, 1927–1940.